

Traction and Wear Evaluation of a Number of Plastic Materials and Greases under
Combined Rolling and Sliding Contact Conditions

Thesis

Presented in Partial Fulfillment of the Requirements for the Degree Master of Science in
the Graduate School of The Ohio State University

By

Steve Wilson, B.S.

Graduate Program in Mechanical Engineering

The Ohio State University

2012

Thesis Committee:

Dr. Ahmet Kahraman, Advisor

Dr. Carlos Castro

ABSTRACT

In this study, a family of experimental evaluations is performed to rank order various combinations of plastic materials and greases for their suitability for automotive auxiliary drive applications in terms of their friction and wear performances. The tests included three common plastic materials (PA46 with 30% glass fiber filler, PA66 with 30% glass fiber filler, and PEEK with 30% carbon fiber filler) and four different proprietary greases. A twin-disk set-up is employed to test plastic disk specimens against a steel roller for their traction characteristics as a function of the slide-to-roll ratio and their wear performance as a function of loading cycles. Friction and wear test results from all twelve plastic-grease combinations are compared to determine particular combinations that provide the best combined wear and traction performance. Results indicate that grease type has a great influence on the friction of the contact, with two of the greases resulting in drastically lower friction coefficients. The PEEK material is found to be the best in terms of its wear resistance. PA46 and PA66 materials with proper grease selection exhibit friction values that are better than PEEK while their wear depths are two to three times that of PEEK.

DEDICATION

This work is dedicated to my family and Amanda for all of their support during my education.

ACKNOWLEDGEMENTS

First and foremost, I would like to thank Dr. Kahraman for his guidance and support throughout this project. I would also like to thank Dr. Sheng Li for helping edit this thesis and Sam Shon for help with the test machine. Lastly, I'd like to thank Honda for their sponsorship of my project.

VITA

September 11, 1989.....Born – Euclid, Ohio
2008.....Engineering Internship, Avery Dennison
2009 – 2010.....Engineering Internship, Babcock & Wilcox NOG-E
2011.....B.S. Mechanical Engineering, The Ohio State University
2011 – 2012.....Graduate Research Associate, The Ohio State University

FIELDS OF STUDY

Major Field: Mechanical Engineering

TABLE OF CONTENTS

	<u>Page</u>
Abstract	ii
Dedication	iii
Acknowledgements	iv
Vita	v
List of Figures	viii
List of Tables	xii
Nomenclature	xiii
<u>Chapter</u>	
1. Introduction	1
1.1 Background and Motivation	1
1.2 Literature Survey	3
1.3 Thesis Objectives	5
1.4 Thesis Outline	6
2. Test Methodology	8
2.1 Twin-Disk Test Machine	8
2.2 Test Specimens	13
2.3 Test Procedures	21
2.3.1 Traction Tests	25
2.3.2 Wear Tests	27
2.4 Inspection Procedures	29

<u>Chapter</u>	<u>Page</u>
3. Experimental Results	34
3.1 Traction Tests	34
3.1.1 Repeatability of Traction Measurements	35
3.1.2 Traction Test Results	37
3.2 Wear Tests	47
3.2.1 Wear Test Results	47
3.2.2 Steel Roller Results	70
4. Conclusions	75
4.1 Summary	75
4.2 Conclusions	76
4.3 Recommendations for Future Work	77
References	79

LIST OF FIGURES

<u>Figure</u>	<u>Page</u>
2.1 Twin-disk test machine overall setup	9
2.2 Schematic of twin-disk test machine with roller and disk highlighted [2]	10
2.3 Close-up of contact between roller and disk on the test machine.....	12
2.4 Test chamber with the safety cover installed	14
2.5 Technical drawing for the roller used in this study	15
2.6 Technical drawing for the disk used in this study.....	16
2.7 (a) A steel roller specimen and (b) plastic disk specimen used in this study	18
2.8 Adapter used for disk shown (a) alone, (b) with disk, and (c) opposite side.....	22
2.9 Roller installation procedure showing (a) needle bearing being pressed in, (b) the precision ball bearings being inserted, (c) the roller shaft being pressed in, and (d) the lock washer, nut, and crescent retaining plate used to contain the ball bearings.	24
2.10 An example of bearing torque loss T_b measurement for a five-minute-long traction test at $u_r = 5$ m/s	28
2.11 Profile measurement setup of (a) disk and (b) roller on a gear CMM.....	30
2.12 Measurement of surface roughness profiles of (a) disk and (b) roller	31
2.13 Example of initial surface roughness measurements for (a) PA46, (b) PA66, and (c) PEEK	32
3.1 An example traction measurement for a PA46 disk with Grease A at $F_n = 200$ N, $u_r = 5$ m/s, and $-1 \leq R \leq +1$	36

<u>Figure</u>	<u>Page</u>
3.2 Three repeats of traction curves of PEEK disks at $u_r = 5$ m/s and $F_n = 200$ N with (a) Grease A, (b) Grease B39	39
(c) Grease C and (d) Grease D40	40
3.3 Measured friction coefficient curves for (a) PA46 disks, (b) PA66 disks41	41
(c) PEEK disks at $u_r = 5$ m/s and $F_n = 200$ N42	42
3.4 Measured friction coefficient curves for (a) Grease A, (b) Grease B43	43
(c) Grease C and (d) Grease D at $u_r = 5$ m/s and $F_n = 200$ N44	44
3.5 Profile measurements for PA46 with Grease A at three measurement locations for $u_r = 5$ m/s, $F_n = 500$ N, and $R = -1$48	48
3.6 Profile measurements for PA46 with Grease B at three measurement locations for $u_r = 5$ m/s, $F_n = 500$ N, and $R = -1$49	49
3.7 Profile measurements for PA46 with Grease C at three measurement locations for $u_r = 5$ m/s, $F_n = 500$ N, and $R = -1$50	50
3.8 Profile measurements for PA46 with Grease D at three measurement locations for $u_r = 5$ m/s, $F_n = 500$ N, and $R = -1$51	51
3.9 Profile measurements for PA66 with Grease A at three measurement locations for $u_r = 5$ m/s, $F_n = 500$ N, and $R = -1$52	52
3.10 Profile measurements for PA66 with Grease B at three measurement locations for $u_r = 5$ m/s, $F_n = 500$ N, and $R = -1$53	53
3.11 Profile measurements for PA66 with Grease C at three measurement locations for $u_r = 5$ m/s, $F_n = 500$ N, and $R = -1$54	54

<u>Figure</u>	<u>Page</u>
3.12 Profile measurements for PA66 with Grease D at three measurement locations for $u_r = 5$ m/s, $F_n = 500$ N, and $R = -1$	55
3.13 Profile measurements for PEEK with Grease A at three measurement locations for $u_r = 5$ m/s, $F_n = 500$ N, and $R = -1$	56
3.14 Profile measurements for PEEK with Grease B at three measurement locations for $u_r = 5$ m/s, $F_n = 500$ N, and $R = -1$	57
3.15 Profile measurements for PEEK with Grease C at three measurement locations for $u_r = 5$ m/s, $F_n = 500$ N, and $R = -1$	58
3.16 Profile measurements for PEEK with Grease D at three measurement locations for $u_r = 5$ m/s, $F_n = 500$ N, and $R = -1$	59
3.17 Variation of the measured average wear depth with loading cycles at $u_r = 5$ m/s, $F_n = 500$ N, and $R = -1$ for (a) PA46, (b) PA66	62
(c) PEEK disks	63
3.18 Variation of measured average wear depth with loading cycles at $u_r = 5$ m/s, $F_n = 500$ N, and $R = -1$ for (a) Grease A, (b) Grease B	64
(c) Grease C and (d) Grease D	65
3.19 Changes in R_a values of surfaces with loading cycles for (a) PA46 disks, (b) PA66 disks	66
(c) PEEK disks	67
3.20 Changes in R_a values of surfaces with loading cycles for (a) Grease A, (b) Grease B	68
(c) Grease C and (d) Grease D	69

<u>Figure</u>	<u>Page</u>
3.21 Comparison of steel roller profiles at three locations before and after the entire wear program	71
3.22 Measured variation of the initial R_a value of the steel roller after wear tests using different greases	72

LIST OF TABLES

<u>Table</u>		<u>Page</u>
2.1	Material properties of plastics and the steel used for specimens [22, 24-26]	19
2.2	Lubricant property data for the four greases used in this study.	20
3.1	Measured average friction coefficient $\bar{\mu}$ values for all material-grease pairs tested for $u_r = 5$ m/s and $F_n = 200$ N.....	45
3.2	Measured changes in surface roughnesses during the traction tests	46
3.3	Measured maximum final wear depth values (in μm) for all material-grease pairs tested for $u_r = 5$ m/s, $F_n = 500$ N and $R = -1.0$	73
3.4	Summary of surface roughness measurements during wear test results	74

NOMENCLATURE

<u>Symbol</u>	<u>Description</u>
c	Contact stress variable [23]
C_E	Contact stress variable [23]
d	Contact stress variable [23]
d_1	Roller diameter
d_2	Disk diameter
E_1	Roller elastic modulus
E_2	Disk elastic modulus
F_c	Friction force at contact interface
F_n	Normal load
K_D	Contact stress constant [23]
r_{lc}	Roller circular lead crown
R	Slide-to-roll ratio
R_a	Average of surface roughness
$R_{a,initial}$	Initial average of surface roughness
ΔR_a	Change in average of surface roughness

T_b	Bearing friction torque
T_c	Roller-disk interface friction torque
T_t	Measured disk shaft torque
u_1	Roller surface velocity
u_2	Disk surface velocity
u_r	Rolling velocity
u_s	Sliding velocity
w_1	Roller face width
w_2	Disk face width
α	Contact stress variable [23]
β	Contact stress variable [23]
μ	Contact friction coefficient
$\bar{\mu}$	Average friction coefficient
$(\sigma_c)_{\max}$	Maximum Hertz contact stress
ω_1	Roller angular velocity
ω_2	Disk angular velocity

CHAPTER 1

INTRODUCTION

1.1 Background and Motivation

With continuing advancements in plastics, plastic gears are becoming increasingly viable alternatives to metal gears in many applications. The use of plastic gears is appropriate in applications with (i) relatively low torque requirements because of the much lower tensile modulus of plastics compared to steels and (ii) intermittent operation instead of continuous operation. Advances in plastics including glass and carbon fiber fillers allowed plastics to be used in applications with higher torque capacities than ever before. However, plastic gears do pose certain challenges compared to steel gears including higher coefficients of thermal expansion, sensitivity to humidity, higher wear rates, and lower thermal conductivities. There are also be multiple benefits of plastic gears compared to steel gears in terms of lubricity (of the plastic itself and when used with certain fillers such as molybdenum disulphate), shock resistance, noise reduction, and weight and cost savings.

In the automotive industry, plastic gears are used in many auxiliary drive applications such as electric power steering (EPS), power windows, seat adjusters, windshield wiper drives, sun roofs, and power doors. Many of the auxiliary drive applications employ a small electric motor with a large speed reduction to meet the torque requirements of the application while reducing the weight, size, and power requirements of the drive motor. These applications often use either plastic gear pairs or a plastic gear in mesh with a steel gear pair to accomplish the desired speed reduction (or torque multiplication). The combination of plastic and steel is especially beneficial for worm gear applications where the worm is made of steel while the worm wheel is made of plastic.

In most auxiliary drive systems, solid lubricants are preferred to liquid ones since heat removal is not as important as friction reduction. By choosing the right plastic and grease combination, an auxiliary drive system can be designed to be more efficient and durable. Efficient auxiliary drive systems allow for improved fuel economy in internal combustion engine driven vehicles and increased range for electric vehicles. Electric power steering is of particular importance, since replacing the more traditional hydraulic power steering with EPS greatly improves the efficiency and allows for autonomous driving functions such as park assist [1]. Due to the increasing importance of auxiliary drive system performance, selecting the best possible plastics and greases is an important first step in designing reliable and efficient auxiliary drive systems for the automotive industry.

1.2 Literature Survey

The twin-disk test machine used in this study for measuring the friction and wear of rolling-sliding contact has been used in the past to evaluate performance of steel-steel contacts [2, 3] and ceramic-ceramic contacts [3]. Other studies have also used a twin-disk test setup to test plastic-plastic contacts as well as plastic-steel contacts [4-8]. Pin-on-disk [9-11], face contact [12], ball-on-prism [13], and spur, helical, crossed helical, and worm gear testing [14-19] have all also been used to examine the wear and/or friction characteristics of plastic-plastic and/or plastic-steel contacts under various load and sliding conditions.

Many studies have been performed to measure friction and wear resulting from rolling-sliding contacts of plastics with other plastics (e.g. [4, 5, 9, 12-20]) and the rolling-sliding contact of plastics with steels [6, 7, 9, 11, 15, 16]. Multiple polyamides (nylons) have been evaluated, including PA6 [9, 10, 20], PA12 [20], PA46 [8, 17, 20], and PA66 [4-8, 14, 20]. Also of interest to gearing applications, polyether ether ketones (PEEK) [12, 13, 15-19] and POM [18, 19] have been the focus of various investigations. POM was shown to have a lower coefficient of friction than PEEK when used in crossed helical applications [18], but it was deemed unsuitable for higher strength applications such as automotive auxiliary drives due to its low melting point and low elastic modulus [19].

PA66 with glass fiber filler was shown to have a lower wear rate than unfilled PA66 when used for plastic-steel contact during twin-disk testing [6]. Conversely, PA66 with a glass fiber, carbon fiber, or aramid filler exhibited an increased wear rate than the

unfilled PA66 in plastic-plastic contacts [5], giving evidence of the benefits of a plastic-steel gear pairing. Further evidence for a plastic-steel pairing was provided by Clerico [9] where plastic-plastic contacts were also shown to exhibit more wear than plastic-steel contacts for PA6. The friction coefficient was shown to be greatly reduced with the use of lubricants [10] and with the addition of glass fiber fillers [6].

A study by Kurokawa et al. [15] tested the performance of PEEK using spur gears, concluding that using a steel rather than PEEK mating gear provided superior wear performance. In another study, the same researchers [16] showed that different types of carbon fiber fillers did not affect the wear rate of PEEK for plastic-steel contacts for spur gears. They concluded that the lubricant type does affect the wear performance of PEEK-PEEK contacts [16]. Parallel and antiparallel orientations of carbon fibers, meanwhile, were shown to improve the wear performance for plastic-steel contact compared to unfilled PEEK, while fibers oriented in the normal direction showed increased wear [11]. The same study indicated that glass fibers fillers increased the wear rate in plastic-steel contact for PEEK for all orientations of the fibers [11], pointing to the benefits of carbon fibers compared to glass fibers when used with PEEK.

Research on the performance of the PA46 plastic material is sparse when compared to PA66 or PEEK, despite the similarities between PA46 and the other nylon products such as PA6, PA12, and PA66. Low speed spur gear testing was conducted on carbon fiber reinforced PA46 in a previous study [20] with a lithium type grease. This study concluded that PA46 has higher wear rates than PA6, PA12, and PA66 [20]. However, it was shown that an unfilled PA46 has better wear performance than glass

filled PEEK despite having a much lower elastic modulus [17]. Gordon [8] showed that PA46 could be used at high loads as long as slide-to-roll ratios are modest, with PA46 specimens melting at higher slide-to-roll ratios.

It is hard to draw conclusions from the available literature about the comparative performance of particular plastics. Automotive auxiliary drive applications use gear pairings that can be subjected to high loads and high slide-to-roll ratios and are likely to be lubricated. Much of the previous research has been performed under unlubricated conditions [4-7, 9-11, 13, 14] and low slide-to-roll ratios [6-8]. Perhaps the only published work on plastic performance under higher loads and higher slide-to-roll ratios was Ref. [4], which was limited to unlubricated contacts of PA66. Similarly, a PA46 study [8] considered high load conditions under lubrication, but with very low slide-to-roll ratios. It is evident from the review of the above literature that a comparison of comprehensive wear performances of different plastics under high load and high sliding conditions is lacking, especially for grease lubricated contacts. In addition, there isn't comprehensive data on the friction performance of different plastics with different greases.

1.3 Thesis Objectives

This study focuses on experimentally investigating the traction and wear characteristics of different combinations of plastic materials and greases for use in automotive auxiliary drive applications. Plastic materials present unique problems when

compared to metals in gearing applications because of their low melting points, low elastic moduli, and low thermal conductivity.

The specific objectives of this research study can be listed as follows:

- Develop test and inspection/measurement procedures to evaluate wear and friction performance of plastic specimens.
- Through review of commercial literature, identify sets of plastic materials (with their optimal filler configurations) and commercial greases.
- Design and fabricate specimens made of the plastic materials identified.
- Perform wear tests with different plastic-grease combinations to rank order them based on their wear performance under heavily loaded, combined rolling and sliding contact conditions.
- Perform friction coefficient measurements as a function of sliding velocity to rank order different plastic-grease combinations based on their friction coefficients.

With the reasons for their selection explained in the next chapter, three plastic materials will be considered in this study: PA46 with 30% glass fiber filler, PA66 with 30% glass fiber filler, and PEEK with 30% carbon fiber filler. In addition, four different greases, named Greases A to D in this study for proprietary reasons, will be considered, forming 12 different plastic-grease combinations.

1.4 Thesis Outline

Chapter 2 presents the details of the test methodology for evaluating friction and wear characteristics of different combinations of plastics and greases in contact with a steel mating surface. An overview of the twin-disk test machine, including detailed descriptions of its mechanical components, the control system, and the data acquisition unit will be given. Mechanical and material properties of candidate plastic materials and greases will be provided. Surface roughness and wear measurement procedures will be described.

Chapter 3 defines the test matrix used for traction testing. The friction coefficient curves from all twelve material-grease combinations are presented individually and are then compared to each other directly. Chapter 3 also describes the test matrix used for wear testing. Wear test results are presented in different forms to assess the wear performance of each plastic-grease combination. These forms include the measured wear depth and changes to the surface roughness profiles.

Finally, Chapter 4 summarizes the traction and wear test results, draws conclusions based on the experimental results, and lists recommendations for future work in this area.

CHAPTER 2

TEST METHODOLOGY

2.1 Twin-Disk Test Machine

The twin-disk test machine, shown in Figure 2.1, was used in this study to evaluate the friction and wear performance of different combinations of plastic materials (three types) and grease lubricants (four types). The schematic view of the machine, shown in Figure 2.2, is designed to push a pair of disks against each other and rotate them in relative sliding. Here, the disk with smaller diameter will be called the *roller* and the disk with larger diameter will be named simply the *disk*. The roller and disk were driven by independent 3 phase AC motors, which were connected to the disk and roller shafts through 2:1 ratio timing belt drives. The motors were each 10 horsepower with a maximum speed of 5,000 rpm. The precise control of the speed outputs of the two motors is achieved by using two identical motor controllers with built in Proportional-Integral-Derivative (PID) control modules along with a LabVIEW control program. Such

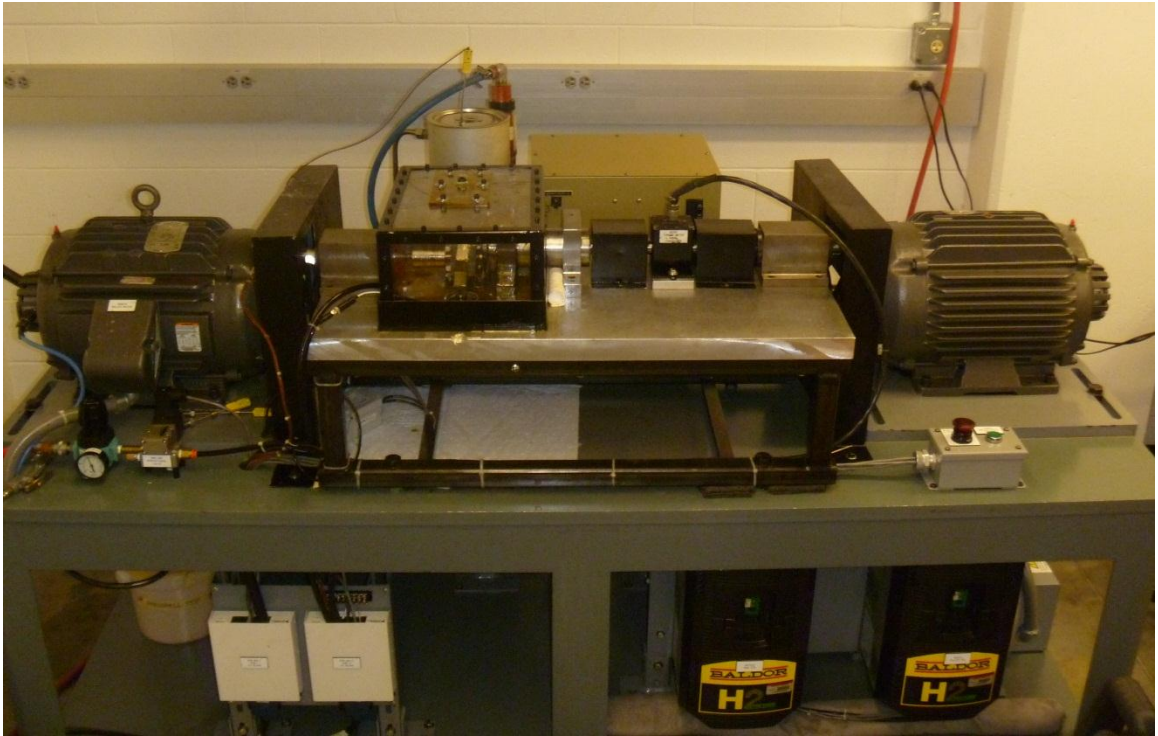


Figure 2.1 Twin-disk test machine overall setup.

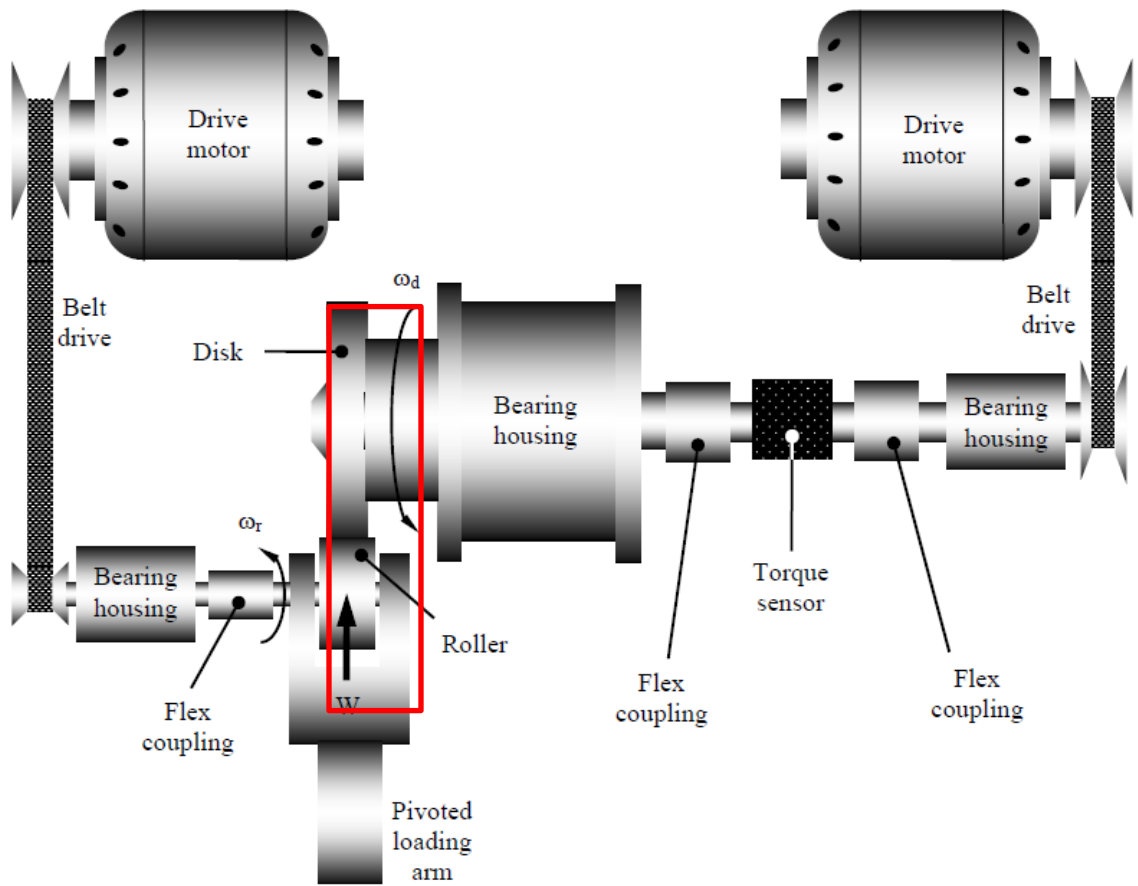


Figure 2.2 Schematic of twin-disk test machine with roller and disk highlighted [2].

independent speed controllers allow precise control of the rolling and sliding speeds of the contact interface. The input shaft (connecting the left-side belt to the roller) and the output shaft (connecting the right-side belt to the disk) are supported by relatively rigid bearings within the bearing housings.

Figure 2.3 displays the close-up view of the roller and disk in contact. The roller was pressed onto its shaft. The roller shaft was supported on one side by a pair of high precision ball bearings and on the other side by a needle bearing in order to ensure consistent axially positioning. In order to accommodate a small amount of play of the roller, a flexible coupling was also used in the connection of the input shaft and the roller shaft as shown in Figure 2.3. The disk was fixed against a shoulder on the output shaft using a steel adapter. The disk shaft is supported by four ball bearings and a needle thrust bearing.

The normal force of the contact was applied through a pivoted loading arm (Figure 2.2) which was pushed against the disk by a pneumatic cylinder. The pressure regulator that connects to the cylinder provides the air pressure up to 550 kPa, corresponding to the maximum normal load of 4,450 N. The applied normal force was measured and monitored using a load cell (Delta Metrics, model XLC86-0250 with a capacity of 1,112 N) which was installed between the loading arm and the pneumatic cylinder head. For the measurement of the friction torque, a torque meter with the capacity of 7 Nm and a resolution of ± 0.037 Nm was mounted between the disk shaft and the output shaft through two flexible couplings (Figure 2.2). The LabVIEW program was used for the test control. This same test rig set-up was successfully used in several

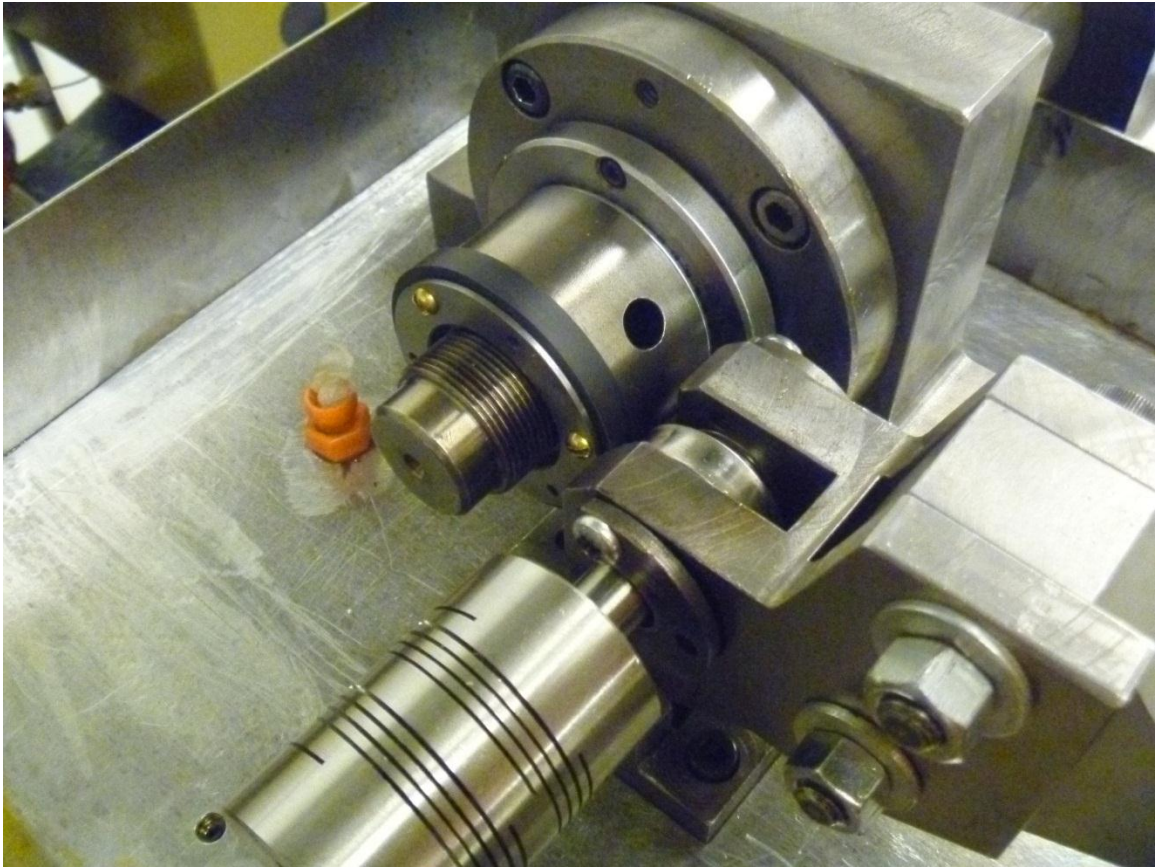


Figure 2.3 Close-up of contact between roller and disk on the test machine.

previous works including ref. [2, 3] in studying the traction and wear characteristics of steel and ceramic materials, respectively.

A sheet metal and Lexan cover was built to enclose the rotating disk and roller to ensure safe operation as seen in Figure 2.4. The cover was also vital, as it contained the grease that was used during testing. In addition, the flex couplings, belt drives, and any other moving components were also contained for safety.

2.2 Test Specimens

For the twin-disk contact pair, the smaller roller was designed as a simple cylinder (without any lead crown) with an outside diameter of $d_1 = 31.75$ mm and a face width of $w_1 = 7.62$ mm. The larger disk had an outside diameter of $d_2 = 57.15$ mm and a face width of $w_2 = 6.35$ mm. Figures 2.5 and 2.6 show the technical drawings of the roller and disk specimens respectively. A circular lead crown of $r_{lc} = 75$ mm radius was also applied for the disk to relieve any effects from edge loading by forming an elliptical contact between the rollers. Since this study focuses on the steel-plastic contact, the roller specimen was made of 4620 steel, which is a typical gear steel. The roller surface was ground and case hardened to the specification of Figure 2.5.

The disk specimens used during this study were made out of three different plastics: PA66 containing 30% glass fiber filler (SABIC RV006ESV_GY7E071), PA46 containing 30% glass fiber filler (Stanyl TW200F6 made by DSM Engineering Plastics), and PEEK containing 30% carbon fiber filler (Victrex PEEK 450CA30). The PA46 and PA66 are polyamides (commonly referred to as nylon). In general, polyamides are known for having a low friction coefficient and favorable wear resistance [21]. PA46 has

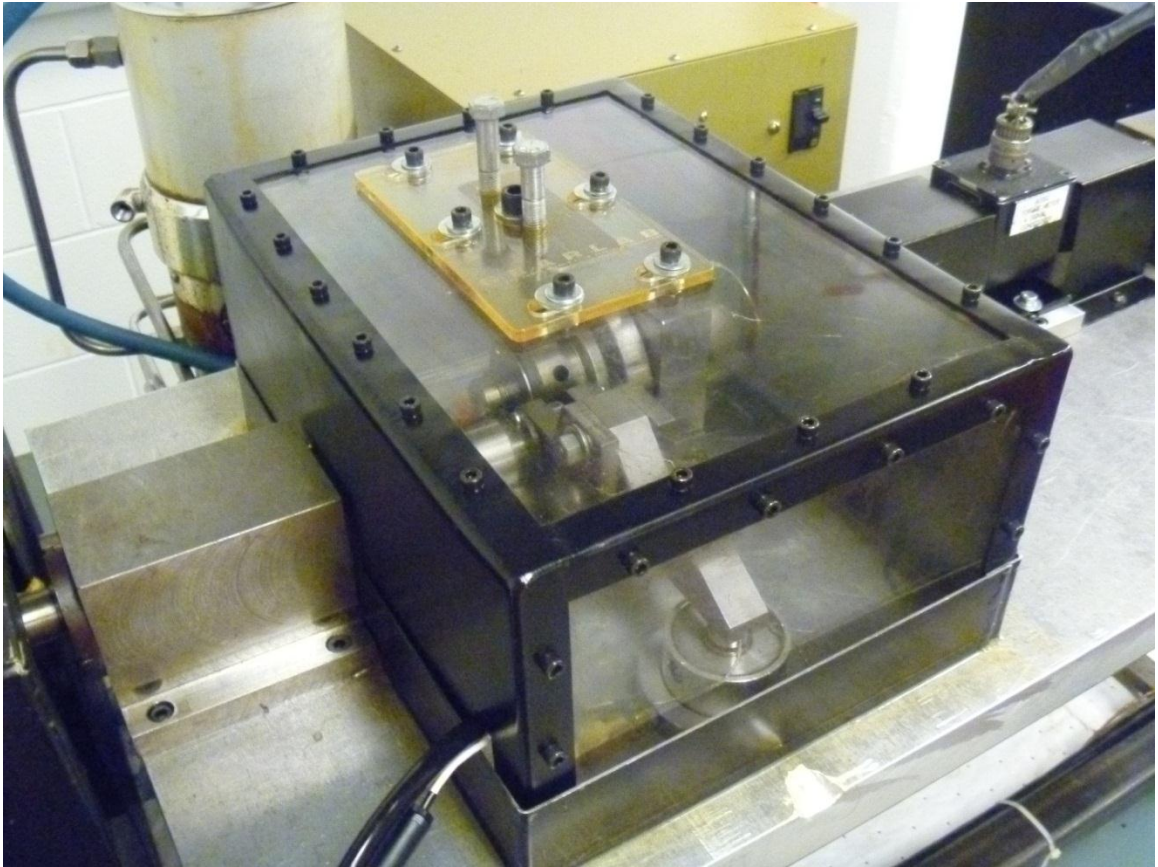


Figure 2.4 Test chamber with the safety cover installed.

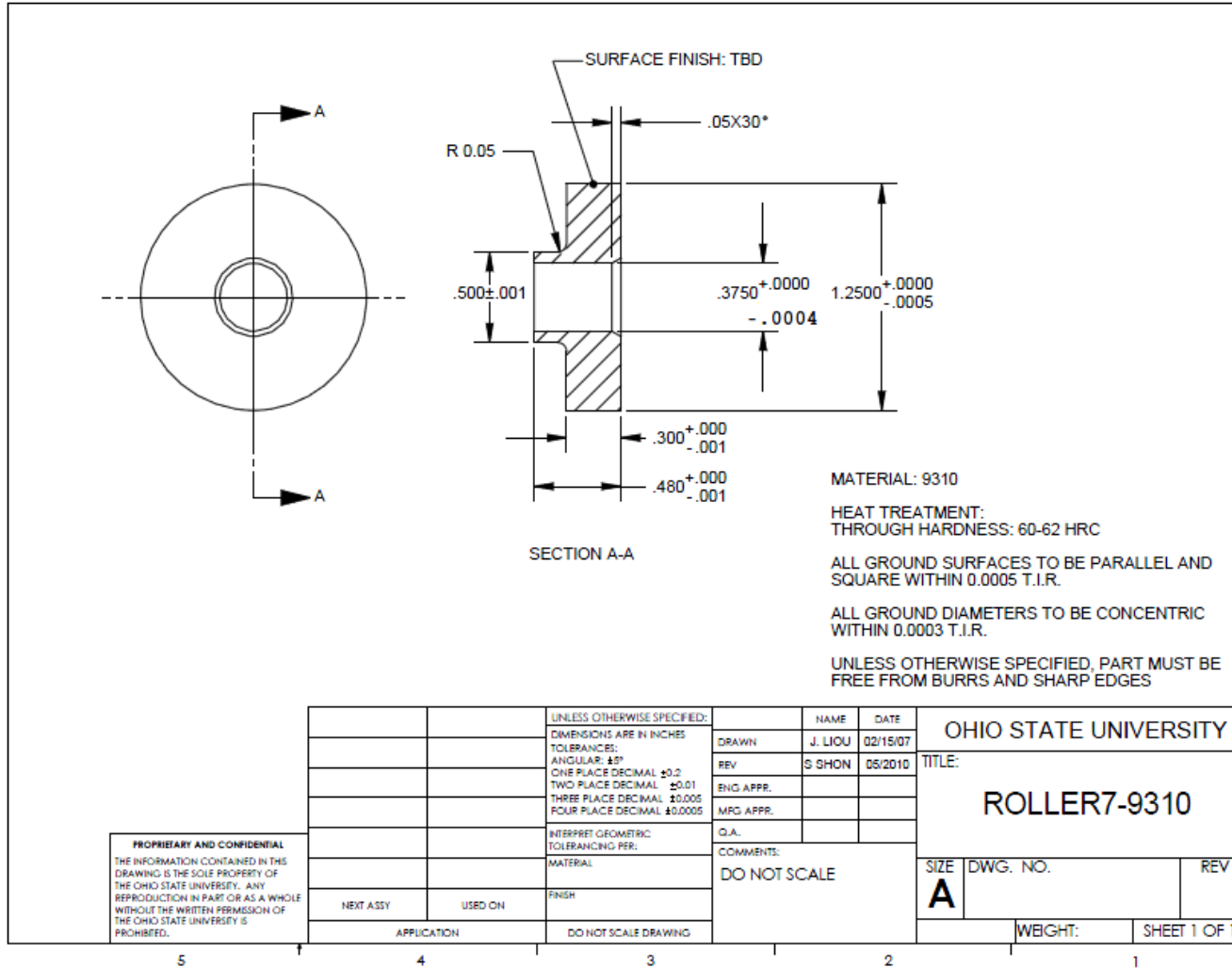


Figure 2.5 Technical drawing for the roller used in this study.

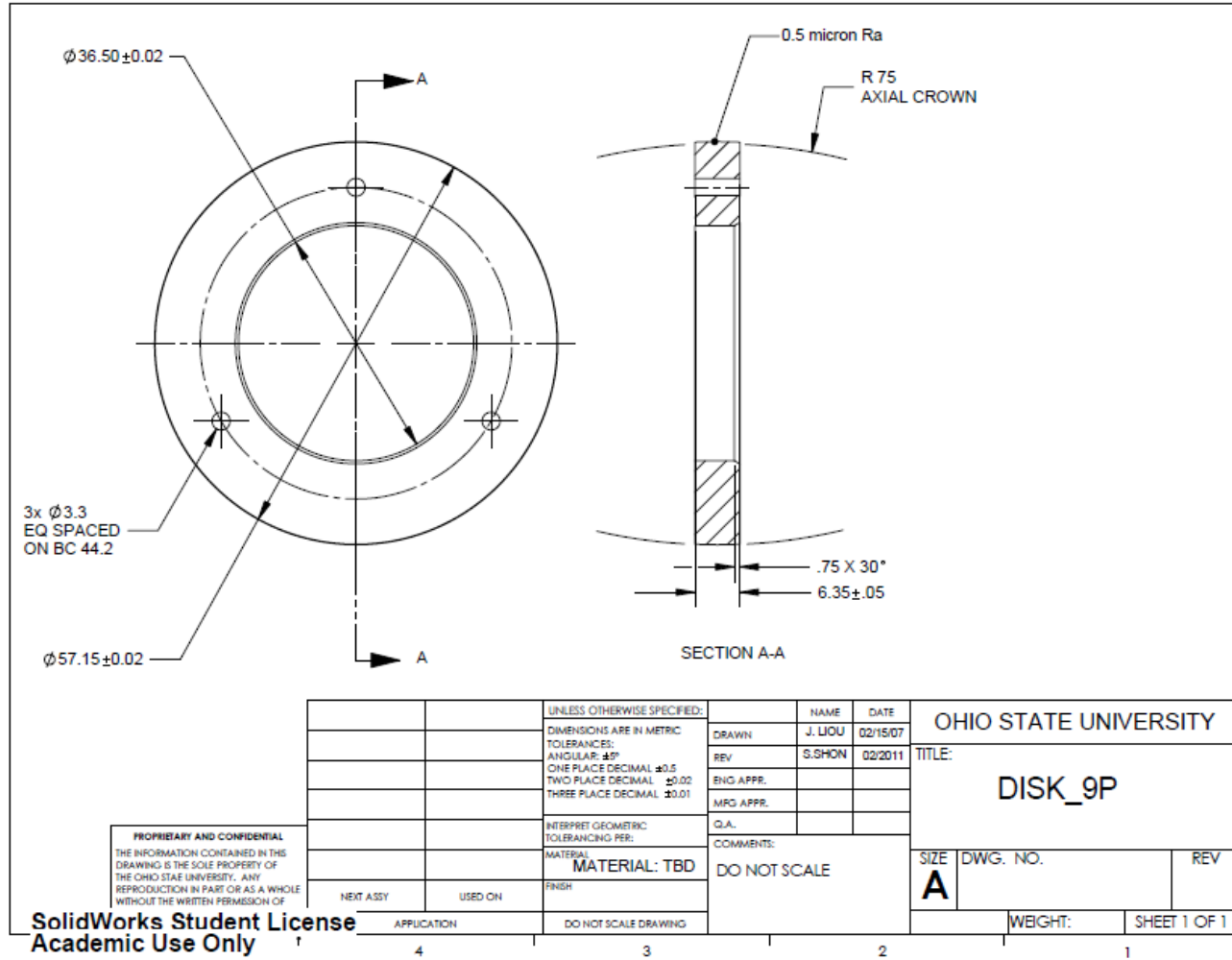


Figure 2.7 Technical drawing for the disks used in this study.

the ability to maintain its mechanical properties at higher temperatures than most other polyamide products since there is a high degree of crystallinity. PA46 also has favorable wear characteristics in gearing applications at higher temperatures compared to other polyamides and PEEK making it one of the candidate materials [17]. In comparison to PA46, PA66 has a slightly higher melting temperature but a much lower tensile strength. PEEK is a polyether ether ketone which is a semi crystalline, thermoplastic material that can be used for injection molding [22]. Compared to the other two plastics, PEEK has enhanced tensile strength and substantially elevated melting temperature. The PA46 and PA66 materials each have glass fiber filler. Glass fibers strengthen the material and can improve other mechanical and thermal properties, but they also increase the friction coefficient and induce wear of the mating surface. The carbon fiber filler in the PEEK is also used for reinforcement and provides a lower coefficient of friction and reduced wear rate compared to glass fibers but at a higher cost [21]. The basic material properties of the three plastic materials and the steel are summarized in Table 2.1. The disk and roller specimens are shown in Figure 2.7.

For the lubrication of the steel-plastic contact, four different greases were selected for this study. They will be referred to as Greases A-D for proprietary reasons and the basic material properties are shown in Table 2.2. Grease A is a lithium soap thickened, medium viscosity synthetic hydrocarbon grease specifically designed for use under high loading conditions. Grease B is also designed for a higher load carrying capacity and designed for good compatibility with plastic materials. Grease C is a lithium soap grease composed of several solid lubricants in a synthetic base oil of polyalphaolefin (PAO). Grease C was specifically designed for applications with plastic to metal contact. The



(a)



(b)

Figure 2.7 (a) A steel roller specimen and (b) plastic disk specimens used in this study.

Table 2.1 Material properties of plastics and the steel used for specimens [22, 24-26].

Property	Units	PA46	PA66	PEEK	4620 Steel
Density	g/cm ³	1.41	1.39	1.40	7.85
Elastic Modulus	GPa	10.0	8.3	25.0	205
Poisson's Ratio	--	0.35	0.35	0.35	0.29
Tensile Strength	MPa	210	162	240	802
Melting Temperature	°C	295	298	343	1421

Table 2.2 Lubricant property data for the four greases used in this study.

Property	Units	Grease A	Grease B	Grease C	Grease D
Kinematic Viscosity (40°C)	cSt	94	150	90	--
Kinematic Viscosity (100°C)	cSt	14	20	unlisted	--
Base	--	Polyalphaolefin	Polyalphaolefin	Synthetic Hydrocarbon Oil	--
Thickener/ Additives	--	Lithium Soap	Lithium Complex	Lithium soap/ PTFE	--
Recommended Temperature Range	°C	-40 to 125	-40 to 350	-45 to 150	--
Color	--	Green	Grey	White	Grey

final lubricant, Grease D, is an experimental grease for which detailed properties are not available.

Since the twin-disk test machine was designed for steel specimens, an adapter had to be machined so that the disk could be mounted without slip occurring between the disk and the disk shaft. The adapter, shown in Figure 2.8, was designed to fit onto the disk shaft without being heated (as is done with steel disk specimens) and was designed to have the plastic disks pressed on with very little force. There were six evenly spaced holes on the adapter, but only three of them were used to mount the disk and adapter to the disk shaft.

2.3 Test Procedures

The physical setup of the traction tests and wear tests was the same, with the plastic disk and steel roller being mounted to their respective shafts. The first step was to press the disk onto the adapter, as shown in Figure 2.8. All of the PA46 and PA66 disks could be pressed onto the adapter without using any tools, but some of the PEEK disks had slightly undersized bores and had to be pressed onto the adapter using a small amount of force with an arbor press. Next, the disk and adapter were placed onto the output shaft with the disk resting directly against the shaft as shown in Figure 2.3. The disk and adapter were secured to the output shaft with three M5 machine screws that passed through three evenly spaced holes on the disk and adapter into tapped holes on the shoulder of the output shaft.

The roller was installed onto the pivoted loading arm while the loading arm was removed from the twin-disk test machine. A needle roller bearing was lightly pressed



(a)



(b)



(c)

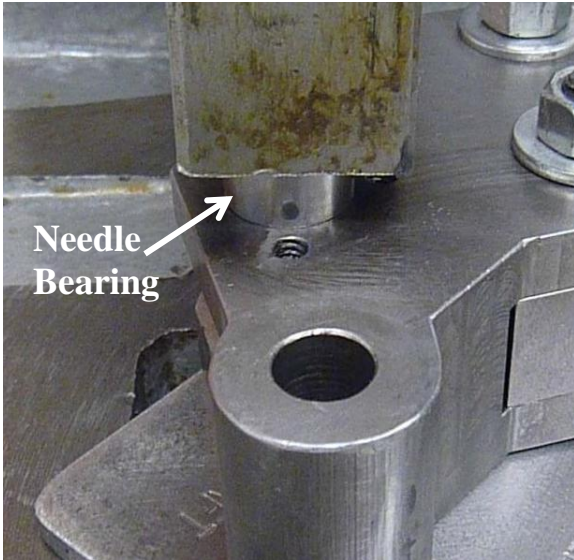
Figure 2.8 Adapter used for disk shown (a) alone, (b) with disk, and (c) opposite side.

into one side of the loading arm as seen in Figure 2.9(a). Next, the two precision ball bearings which supported the opposite side of the roller shaft were placed into the pivoted loading arm as seen in Figure 2.9(b). The ball bearings had a clearance fit with the loading arm allowing the roller shaft to move axially. The roller shaft was then pressed, using a small arbor press, through the installed needle bearing, roller, and ball bearings until the shoulder of the roller shaft rested tightly against the roller. A lock washer and nut were tightened onto the end of the roller shaft, against the inner race of the outer ball bearing to prevent any axial motion of the shaft with respect to the ball bearings as seen in Figure 2.9(c). Lastly, two crescent shaped retaining plates were installed to securely house the assembled roller shaft as seen in Figure 2.9(d).

The loading arm (with the load cell and roller shaft attached) was installed onto the twin-disk test machine using a pin to allow the loading arm to pivot. A flexible coupling was used to attach the roller shaft to the input shaft. After the roller and disk were aligned correctly, the flexible coupling was tightly secured, preventing axial motion of the roller shaft and fixing the input and roller shafts together.

2.3.1 Traction Tests

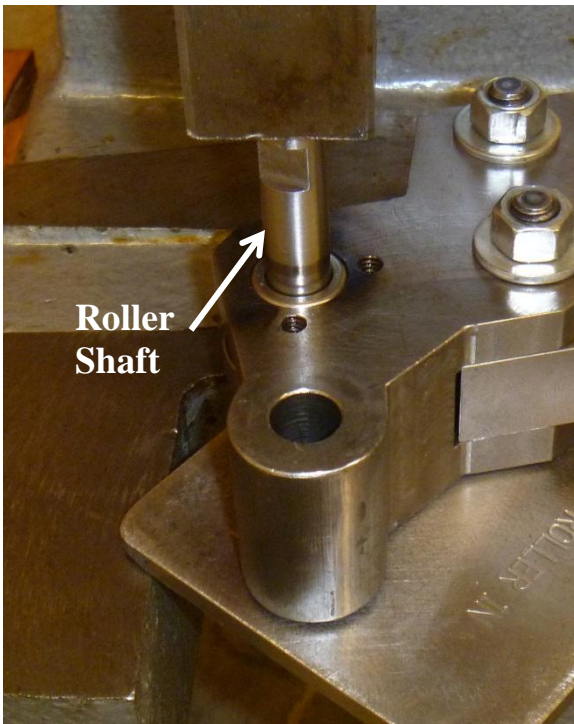
Traction tests were performed in order to determine the friction characteristics for all of the combinations of greases and plastics. In these tests, the rotational speeds of roller (ω_1) and the disk (ω_2) were varied in a simultaneous manner to achieve uniformly changing surface velocities $u_1 = \frac{1}{2}d_1\omega_1$ and $u_2 = \frac{1}{2}d_2\omega_2$. Defining rolling (mean) and sliding velocities of the contact, respectively, as



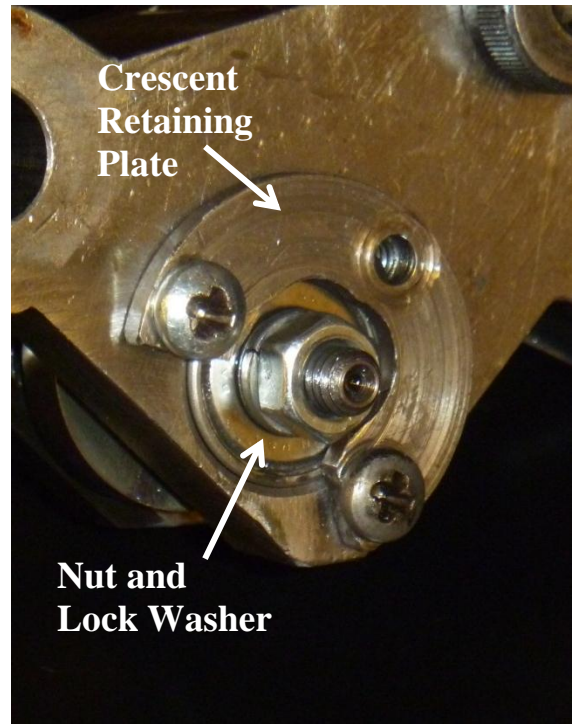
(a)



(b)



(c)



(d)

Figure 2.9 Roller installation procedure showing (a) needle bearing being pressed in, (b) the precision ball bearings being inserted, (c) the roller shaft being pressed in, and (d) the lock washer, nut, and crescent retaining plate used to contain the ball bearings.

$$u_r = \frac{1}{2}(u_1 + u_2), \quad (2.1)$$

$$u_s = u_1 - u_2. \quad (2.2)$$

With the slide-to-roll ratio defined as $R = u_s/u_r$, different sliding conditions can be achieved using different u_1 and u_2 (in other words, ω_1 and ω_2) values. For instance, a negative 100% sliding condition, i.e. $R = -1.0$ requires that $u_1 = \frac{1}{3}u_2$. Likewise, $R = 1.0$ corresponds to $u_1 = 3u_2$. In a traction test, the same u_r value and normal load F_n are maintained while R is varied from $R = -1.0$ to $R = +1.0$ by changing u_1 and u_2 in relation. For the traction measurements, $F_n = 200 \text{ N}$ and $u_r = 5 \text{ m/s}$ values were used. Using the Hertzian contact formulae for the maximum stress $(\sigma_c)_{\max}$ of two bodies in elastic contact the maximum contact stress is calculated as

$$(\sigma_c)_{\max} = \frac{1.5F_n}{\pi cd} \quad (2.3)$$

where,

$$K_d = \frac{1.5}{2/d_1 + 2/d_2 + 1/r_{lc}}, \quad (2.4)$$

$$C_E = \frac{1-\nu_1^2}{E_1} + \frac{1-\nu_2^2}{E_2}, \quad (2.5)$$

$$c = \alpha^3 \sqrt{F_n K_D C_E}, \quad (2.6)$$

$$d = \beta^3 \sqrt{F_n K_D C_E}. \quad (2.7)$$

The contact stresses were calculated using the disk and roller dimensions given in Figures 2.5 and 2.6 and the values for α and β from ref. [23]. The load level of $F_n = 200\text{ N}$ corresponds to the maximum contact stresses of 200 MPa for PA46, 178 MPa for PA66, and 352 MPa for PEEK. A traction test from $R = -1.0$ to $R = +1.0$ was designed to take 5 minutes with the traction torque and normal force sampled at 2 Hz.

For these loaded tests, the measured disk shaft torque T_t consisted of the roller-disk interface friction torque T_c and the bearing friction torque T_b such that

$$T_t = T_c + T_b. \quad (2.8)$$

As the main interest is the measurement of the contact friction coefficient

$$\mu = \frac{F_c}{F_n} \quad (2.9)$$

where $F_c = 2T_c/d_2$ is the friction force at the contact interface, one must isolate T_c from T_b according to Eq. (2.8). For this purpose, a traction test with zero normal load was performed before each set of loaded tests such that $T_c = 0$ and $T_t \approx T_b$. It is found that the bearing torque is linearly-dependent on the slide-to-roll ratio as shown in an example measurement in Figure 2.10. The T_b value at each R value was then subtracted from the measured T_t values at the same R value from a loaded test to determine T_c to be used in Eq. (2.9) to determine μ .

The unloaded test was performed before every different combination of plastic and grease in order to ensure the accuracy of the bearing loss compensation. The bearing

losses did not change significantly between tests, but as the bearings aged it was important to ensure that the bearing compensation remained accurate. In order to reduce the measurement error, the traction test was performed three times for each plastic-grease combination. The three tests were then averaged to obtain a representative friction coefficient curve for each material-grease combination. Figure 3.2 in the Experimental Results chapter shows an example set of measurements taken for PEEK and Greases A-D.

2.3.2 Wear Tests

A test procedure was developed to quantify the wear performance of every plastic material and grease combination defined in the test matrix. Since the plastic disks were expected to wear at a significantly higher rates than the mating steel rollers, a sliding ratio of $R = -1.0$ was used in wear tests to allow the disk speed and the wear cycles to be maximized. This made it possible to complete wear tests within a reasonable period of time.

The normal force was maintained nominally at $F_n = 500\text{ N}$ during the tests for all of the materials and grease combinations. The material properties of the plastics vary significantly, so the contact stress (which strongly influences wear) was different for the different materials. The contact stress was 271 MPa for PA46, 241 MPa for PA66 and 477 MPa for PEEK. However, in practical gearing applications the design would specify a torque value to be transmitted regardless of the material choice. The torque requirement in a gearing application is consistent with comparing the materials using a constant normal load rather than a constant contact stress.

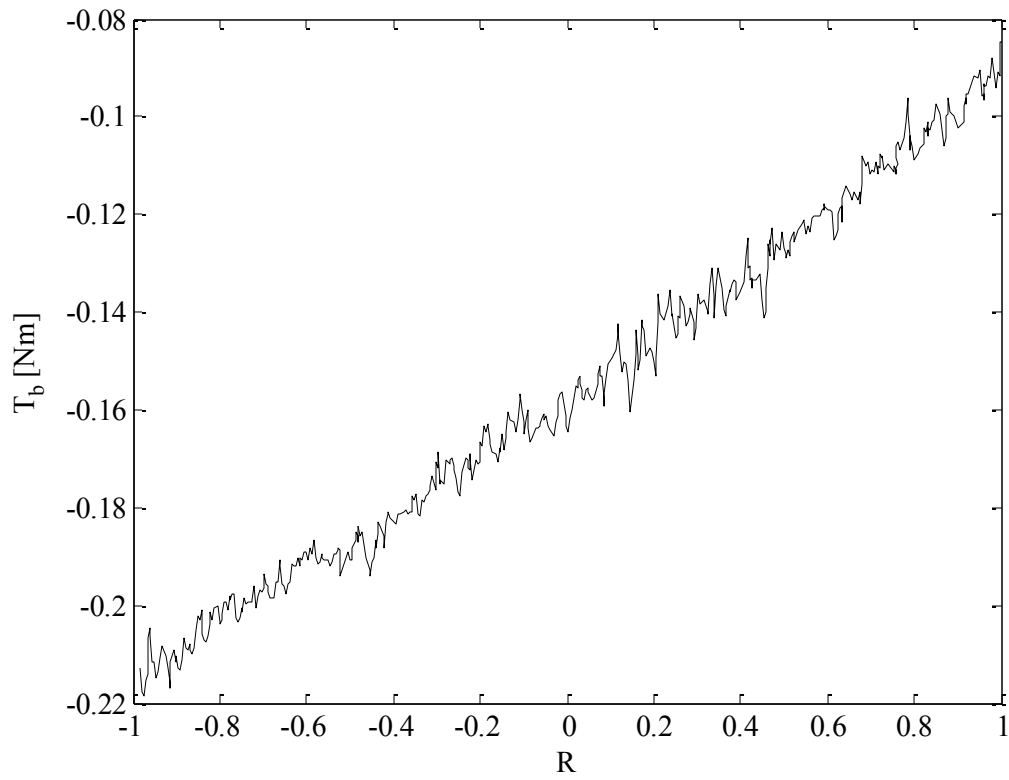


Figure 2.10 An example of bearing torque loss T_b measurement for a five-minute-long traction test at $u_r = 5 \text{ m/s}$.

2.4 Inspection Procedures

All of the test specimens were inspected prior to a new test by measuring the (i) surface roughness profiles in the circumferential direction and (ii) profiles in the axial direction at three equally spaced positions. Figure 2.11(a) and (b) shows the setups for measuring the disk and roller profiles using a Gleason M&M 255 Gear Coordinate Measurement Machine (CMM). The surface roughness is measured separately, as shown in Figure 2.12(a) and (b) for the disk and roller, respectively. A Taylor-Hobson Form Talysurf-120 was used for the surface roughness testing. An example of the surface roughness measurements is shown in Figure 2.13. A cutoff length of 0.8 mm was selected to filter out the surface waviness since the plastic specimens have the roughness amplitudes that are within the range of approximately 0.3 μm to 1.0 μm . Each measurement covered the length of 4mm. Only the centers of the profiles are in contact while testing so the surface roughness should have only been affected in these regions. An effort was made to position the disks and rollers so that the roughness was always measured at the center of the contact region.

Since the traction tests were short, approximately 15 minutes of roller-disk contact time per sample (three tests of five minutes), neither significant surface roughness changes or large scale profile changes were expected to occur. For this reason, the measurements of the disk were taken after all three traction tests were completed rather than testing in between every test. The same roller was used for all of the traction testing and measured periodically to ensure that the surface roughness did not change significantly.



(a)

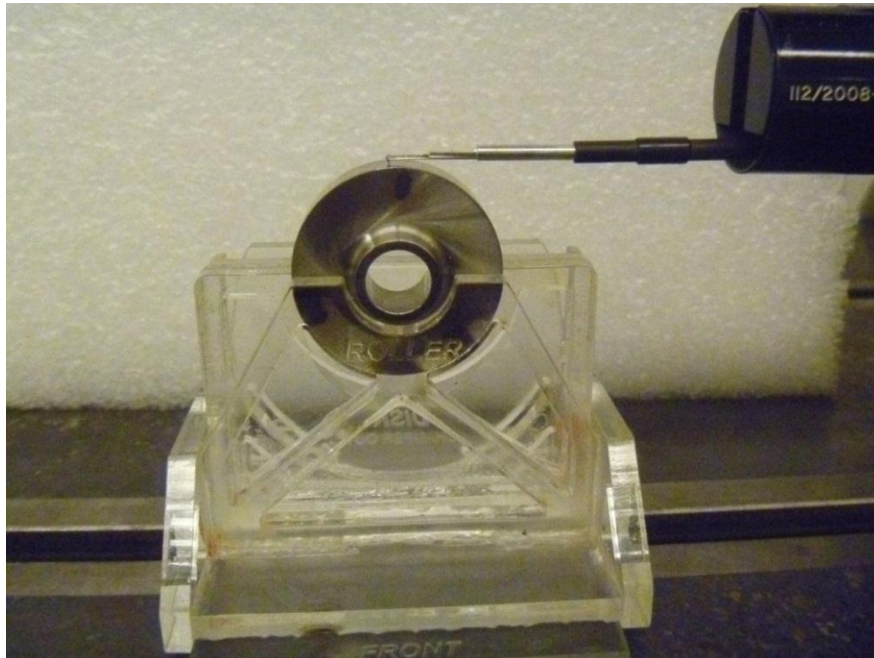


(b)

Figure 2.11 Profile measurement setup of the (a) disk and (b) roller on a gear CMM.



(a)



(b)

Figure 2.12 Measurement of surface roughness profiles of (a) disk and (b) roller specimens.

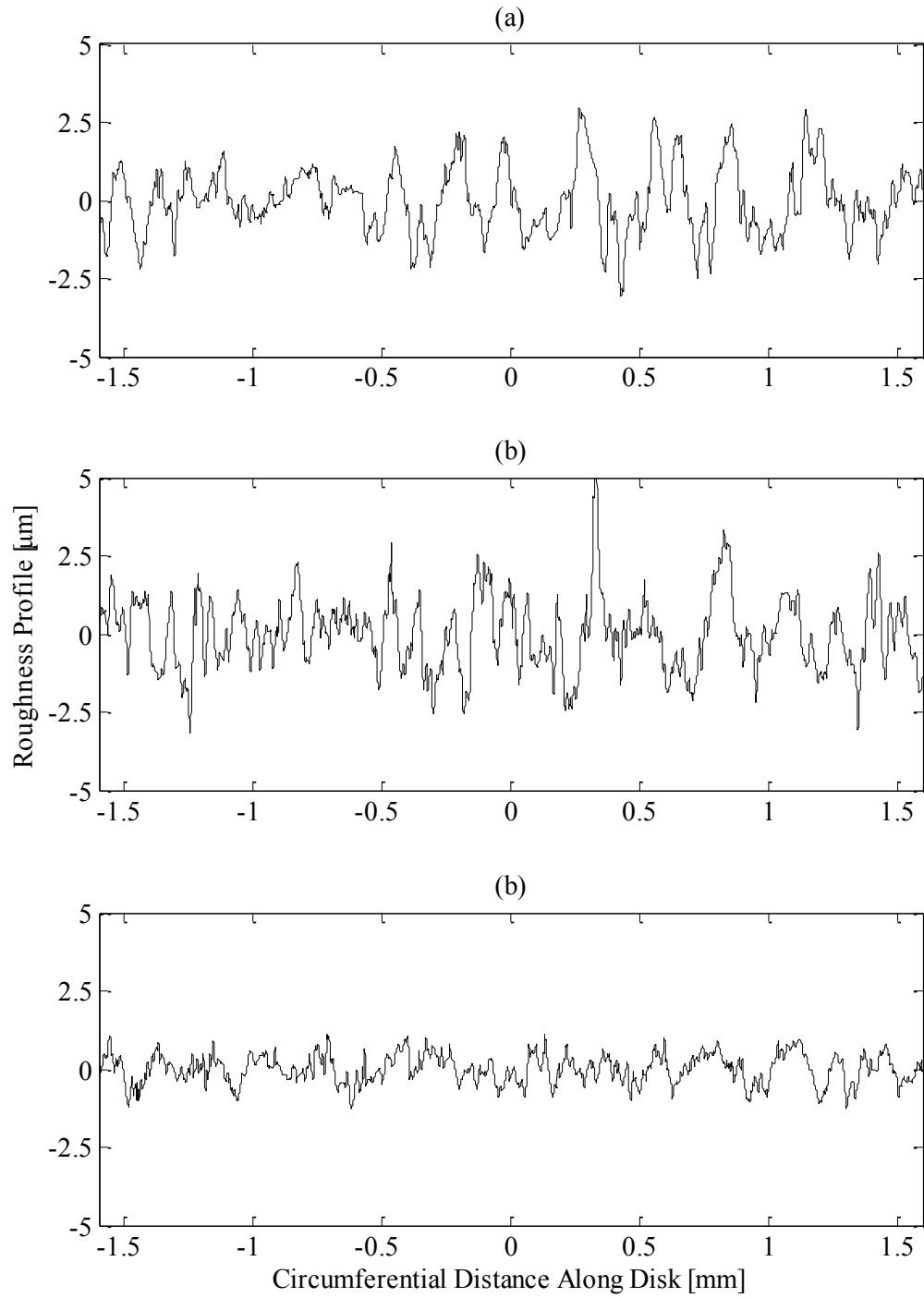


Figure 2.13 Example of initial surface roughness measurements for (a) PA46, (b) PA66, and (c) PEEK.

For the wear tests, a total of 1 million cycles were run for each plastic-grease combination for a total of 245,100 meters of sliding. The surface roughness and profile of the plastic specimens were measured at 0.2 million cycle increments (nearly 163.4 minutes). During the wear tests, the wear of the plastic disks was quantified by measuring the amount of material removed at the center of the disk profile as a function of the number of disk cycles. The profile and surface roughness was measured at three circumferential locations spaced equally around the disk. The roller was also measured periodically, yet less frequently than the disks since the steel wasn't expected to wear significantly.

CHAPTER 3

EXPERIMENTAL RESULTS

3.1 Traction Tests

One of the main criteria for evaluating plastic materials and greases was identified in Chapter 2 as the resultant traction at the contact interface. Measured friction coefficient μ can be used as the metric for the mechanical efficiency of the final gear pair with a particular material-grease combination. In order to assess the contact performance relating to the friction for the different plastic-grease combinations, the test matrix shown was defined taking into account all three materials (PA46, PA66, and PEEK as defined in Table 2.1) and all four greases (A, B, C, and D as defined in Table 2.2). All of the tests for the twelve combinations were run under the same operating conditions with a normal force of $F_n = 200$ N, a rolling velocity of $u_r = 5$ m/s, and a slide-to-roll ratio of $-1 \leq R \leq +1$. These operating ranges are selected according to the typical plastic gear contact conditions from a companion study. With the grease lubricant, the influence of load and speed variations on the friction coefficient is assumed to be small and is out of the scope of this study.

For each traction test, the friction coefficient is measured continuously from $R = -1$ to $R = +1$ over a five-minute time interval. It has been observed that the measurements with negative sliding are significantly smoother and more consistent than those with positive sliding such as the PA46 and Grease A combination shown in Figure 3.1. The oscillations observed in Figure 3.1 for $R > 0$ were found to be due to structural vibrations of the set-up due to the way the rollers are loaded. They were observed in earlier experiments of Liou [2] with the same test setup as well. As the sole purpose of this study was to rank order the plastic material-grease combinations, only the negative side of the sliding ratio range was considered with absolute values applied to R and μ ($|R| = R$ and $|\mu| = \mu$). Also, $-1 < R < -0.8$ is not considered since the excess of grease applied at the beginning of the test is still being removed from the roller-disk interface at these slide-to-roll ratios, giving inconsistent values for μ in this region.

Prior to each traction test, a bearing torque test was performed first and the bearing related losses were removed from each actual traction test. The traction curves shown in the next two sections represent contact traction only with bearing contributions removed.

3.1.1 Repeatability of Traction Measurements

As shown in Figure 2.3, there isn't a housing that encloses the roller pair closely, so the grease applied at the beginning of the test is flung off of the roller and disk surfaces throughout the test, changing the lubrication conditions during the test in the process. One would expect some variability in the data due to other variations as well,

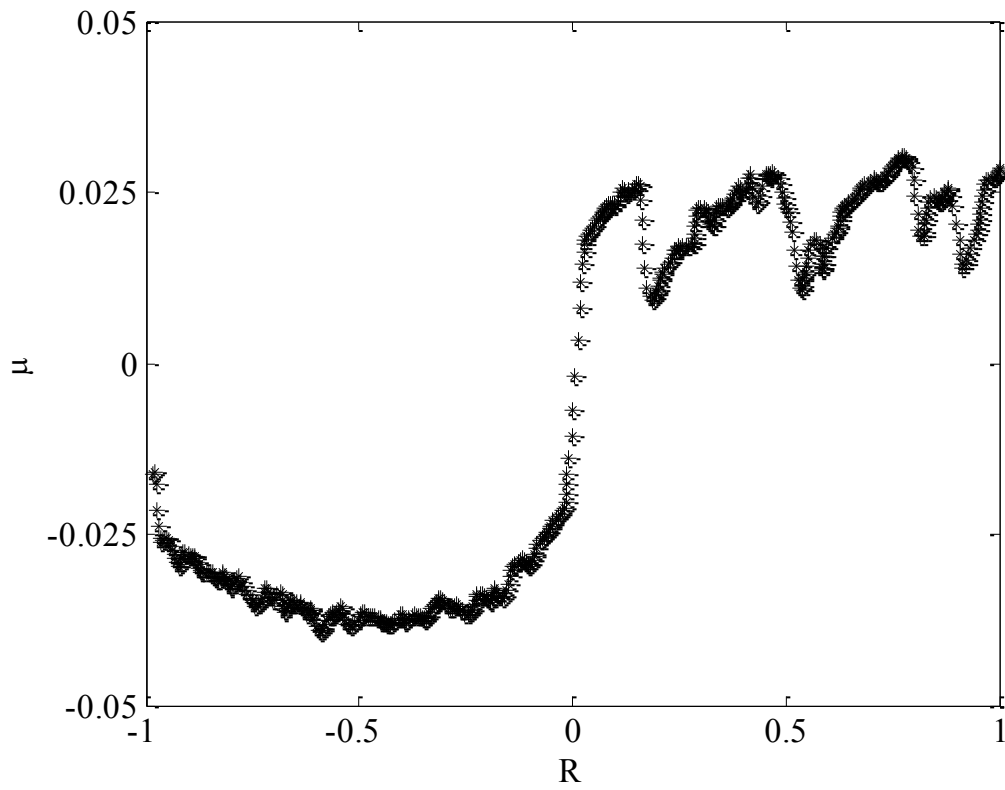


Figure 3.1 An example traction measurement for a PA46 disk with Grease A at $F_n = 200$ N, $u_r = 5$ m/s, and $-1 \leq R \leq +1$.

such as plastic disk surface roughnesses, as well as expected uncertainties associated with the applied normal force F_n and the measured traction torque T_c . In order to demonstrate the extent of such variability, three repeat tests of PEEK disks with each of the four greases are compared in Figure 3.2. Certain amount of variation is evident here especially for Greases A and B. In order to reduce impact of such variability, each test in Table 3.1 was repeated three times and post-processed to represent the average of the three runs.

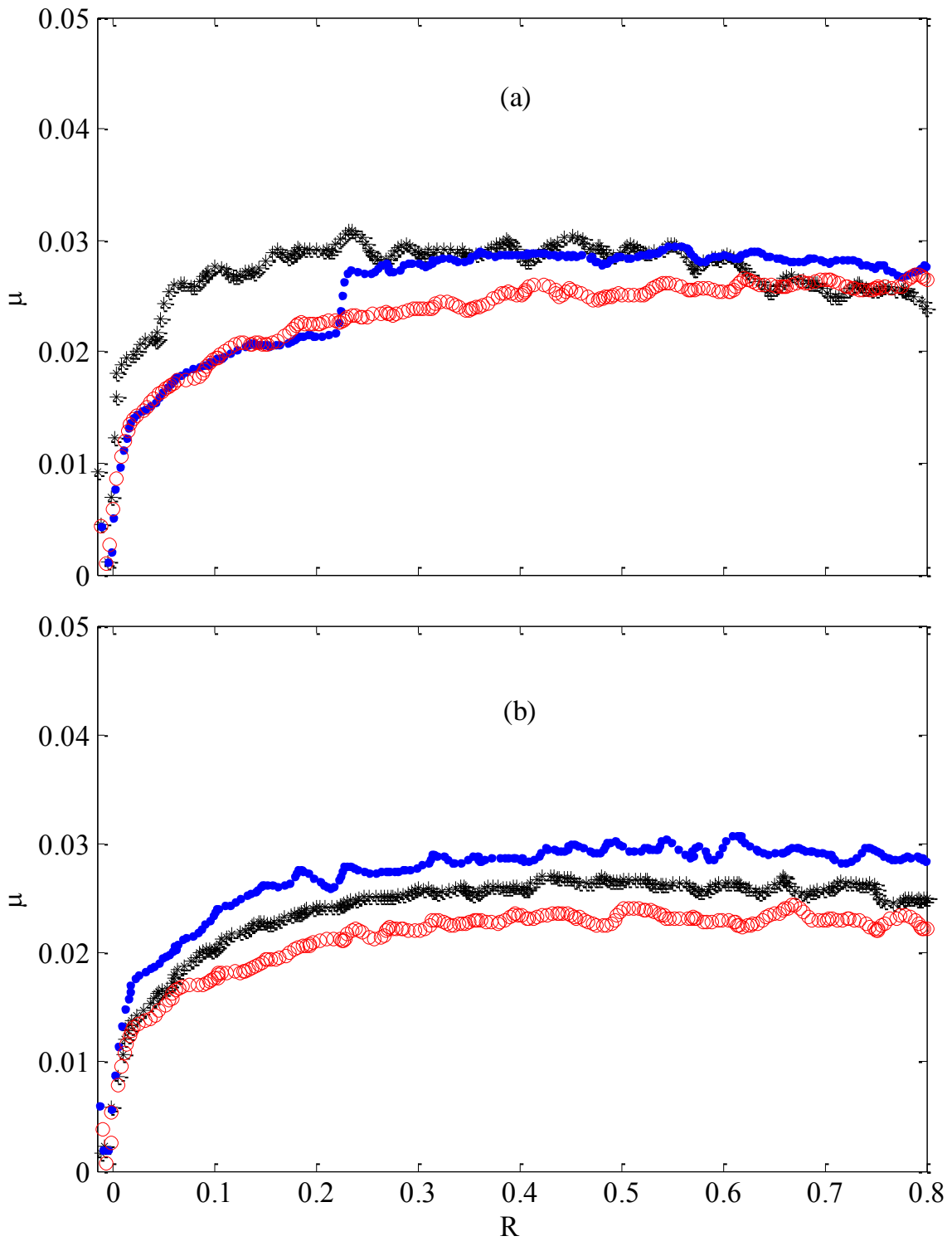
3.1.2 Traction Test Results

In Figure 3.3(a-c), measured traction curves for PA46, PA66 and PEEK, respectively, are compared for all four types of greases. The same data is rearranged in Figure 3.4(a-d) to provide direct material comparisons for each of the four grease types, respectively. Table 3.1 compares lists the average values of the friction coefficients $\bar{\mu}$ (average value of μ within $-0.8 \leq R \leq -0.2$) for all 12 combinations. Based on Figures 3.3, 3.4 and Table 3.1, the following observations can be made in terms of the friction performance of plastic materials and greases considered:

- Overall, PA46 with Grease C was measured to result in the lowest average friction coefficient of $\bar{\mu} = 0.012$ (1.2%).
- The worst case with the highest friction of $\bar{\mu} = 0.037$ (3.7%) was PA66 with Grease A indicating that the material-grease combinations tests represents a spread of about 2.5%.

- It was noted that Grease C is the best choice for PA66 and PA46 while Grease D resulted in the minimum $\bar{\mu}$ values with PEEK.
- Overall, tests with greases A and B resulted in $\bar{\mu}$ values that are nearly two times higher than those with Greases C and D, regardless of material type. Grease D can be identified as the best grease amongst four based on its friction outcome.
- The ranking of the three plastic materials with a particular grease was not consistent as a different ranking was seen with a different grease, pointing to the fact that proper matching of the plastic material and the optimal grease is required.

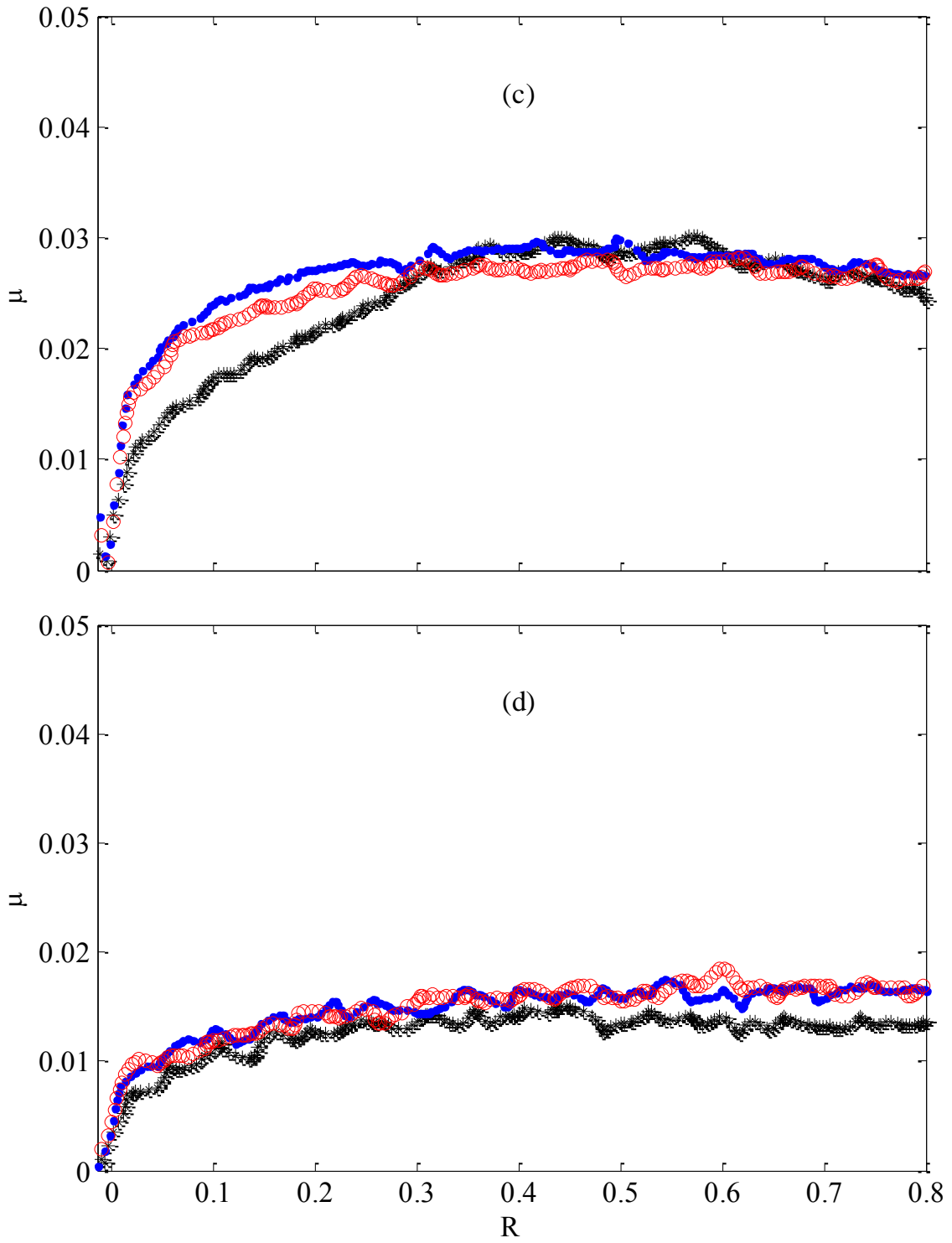
Table 3.2 provides the results of the average surface roughness measurements from the plastic disks before and after the traction tests. As stated in Chapter 2, the machinability of the plastic materials was a criterion used in the selection process. Since each plastic material had different fillers to increase strength and reduce wear, the machined disk surfaces were expected to exhibit varying level of roughness. With R_a values in metric, the surface roughnesses of new PA66 disks (before test) ranged with 0.82 to 0.88 μm . The new PA46 disks had comparable roughness values of $R_a = 0.86 - 0.97 \mu\text{m}$, while the new PEEK disks exhibited much smoother surfaces at $R_a = 0.43 - 0.46 \mu\text{m}$. Table 3.2 also shows that the same surfaces after the 5-minute traction tests became smoother with the reductions in R_a values ranged from 1.3% to 35.5% with no clear sensitivity to any particular material or grease.

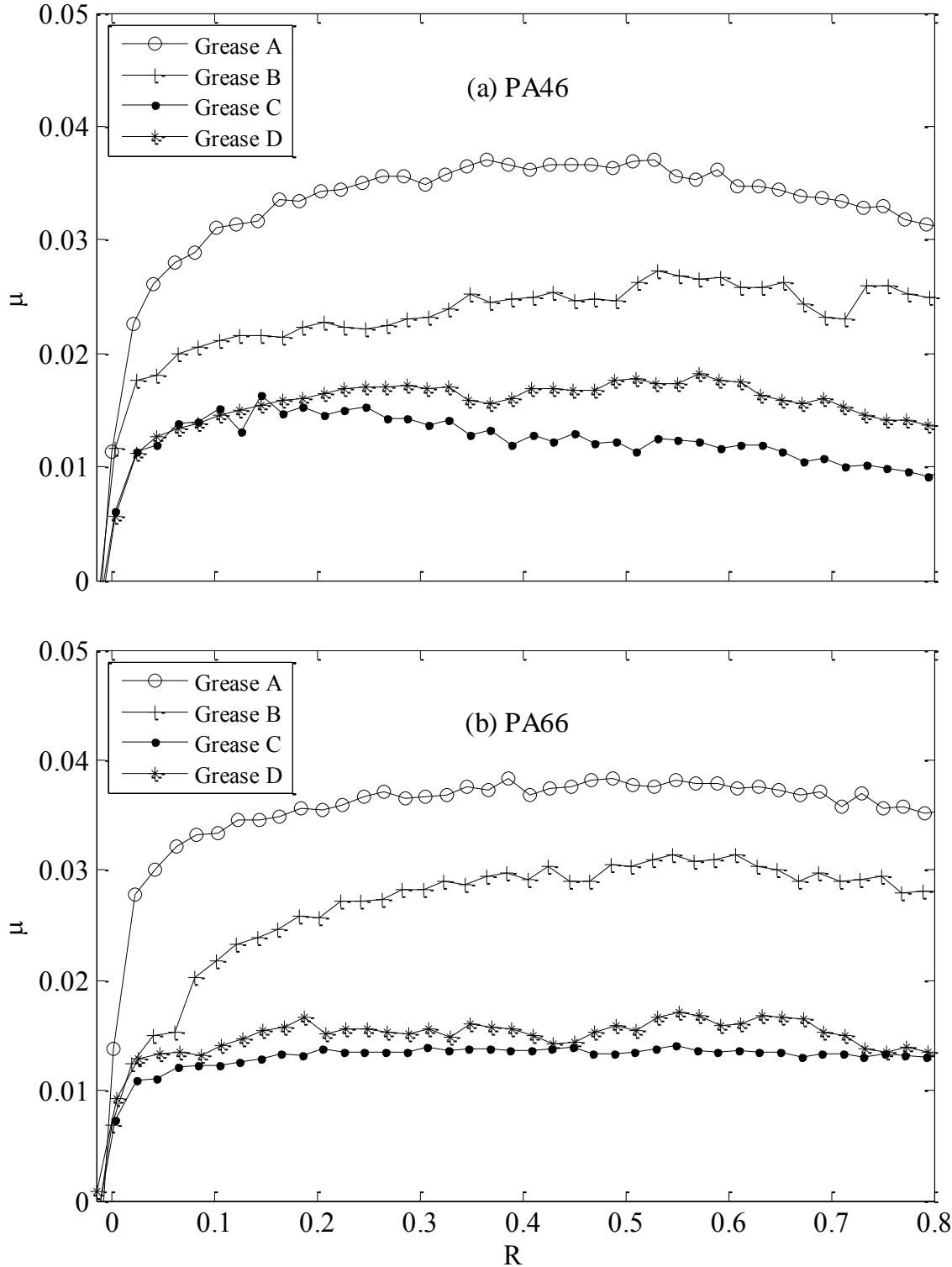


Continued.

Figure 3.2 Three repeats of traction curves of PEEK disks at $u_r = 5$ m/s and $F_n = 200$ N with (a) Grease A, (b) Grease B, (c) Grease C, and (d) Grease D.

Figure 3.2 Continued.

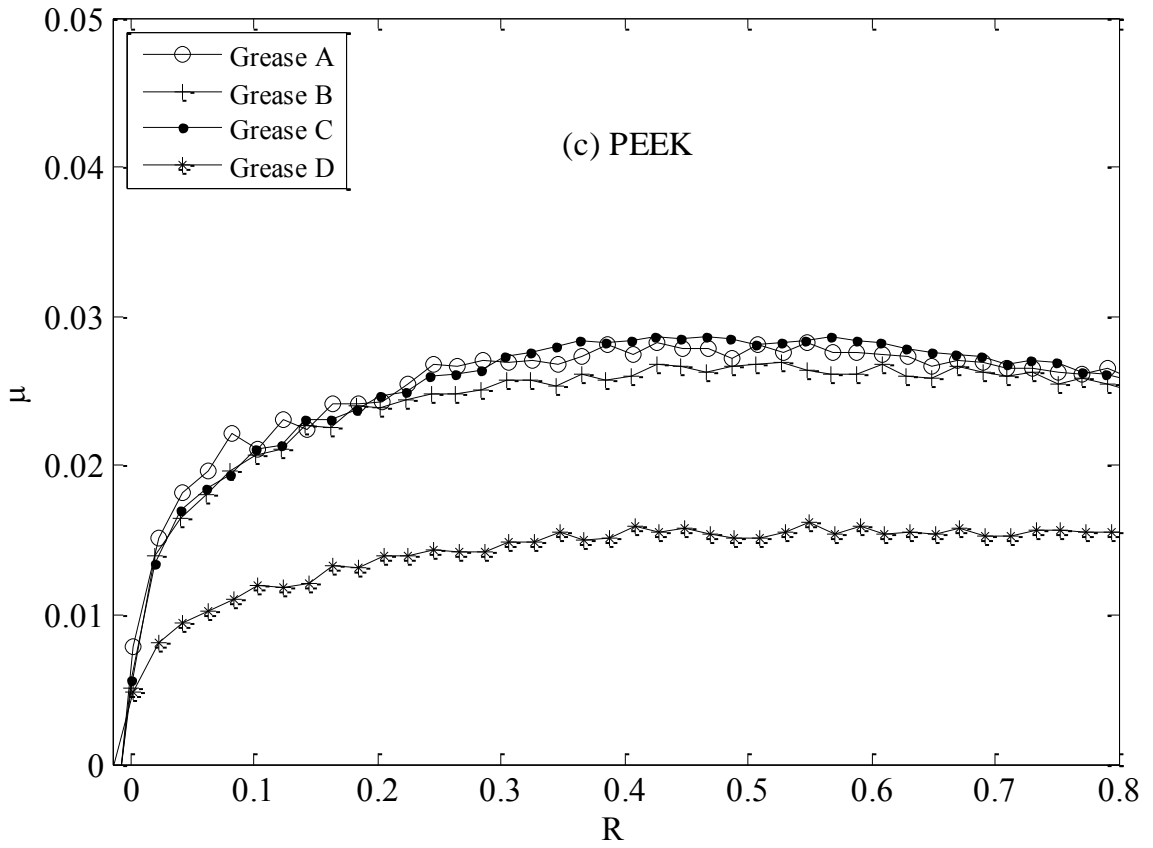




Continued.

Figure 3.3 Measured friction coefficient curves for (a) PA46 disks, (b) PA66 disks and (c) PEEK disks at $u_r = 5$ m/s and $F_n = 200$ N.

Figure 3.3 Continued.



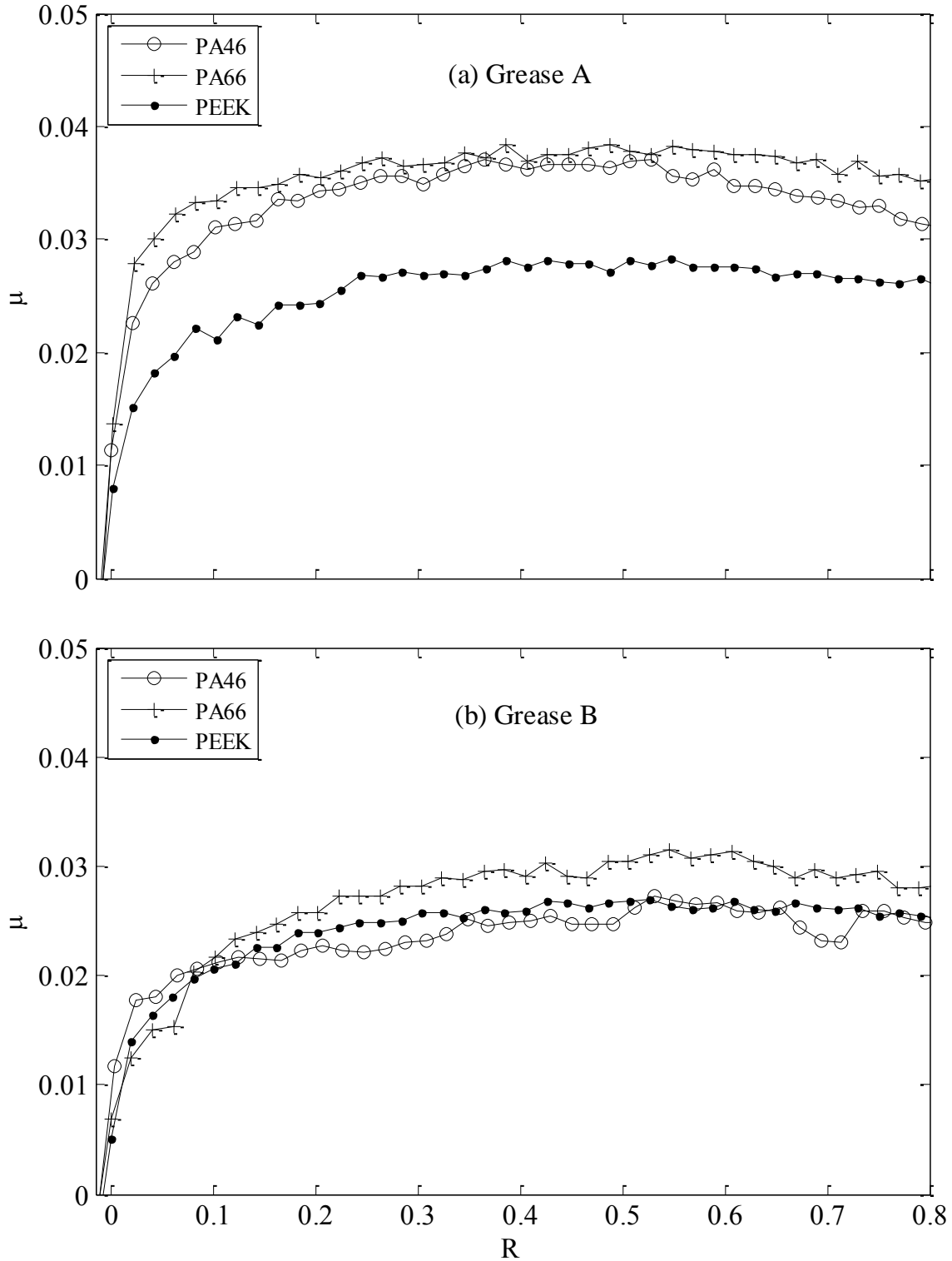


Figure 3.4 Measured friction coefficient curves for (a) Grease A, (b) Grease B, (c) Grease C and (d) Grease D at $u_r = 5$ m/s and $F_n = 200$ N.

Figure 3.4 Continued.

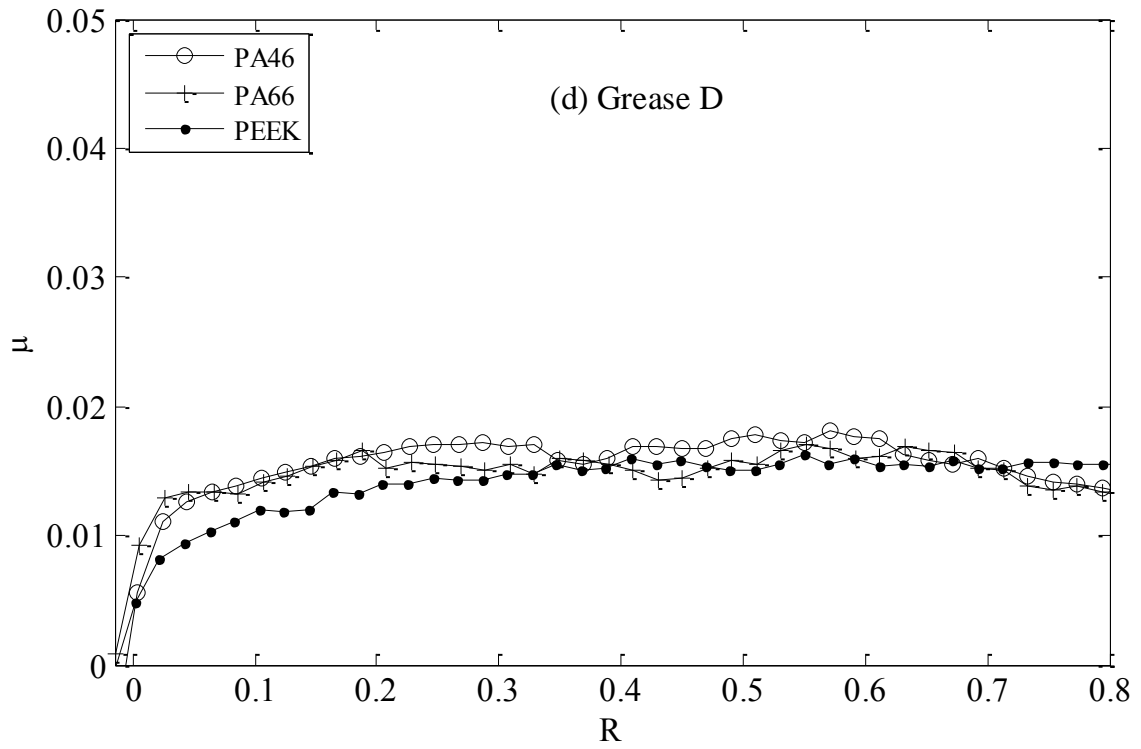
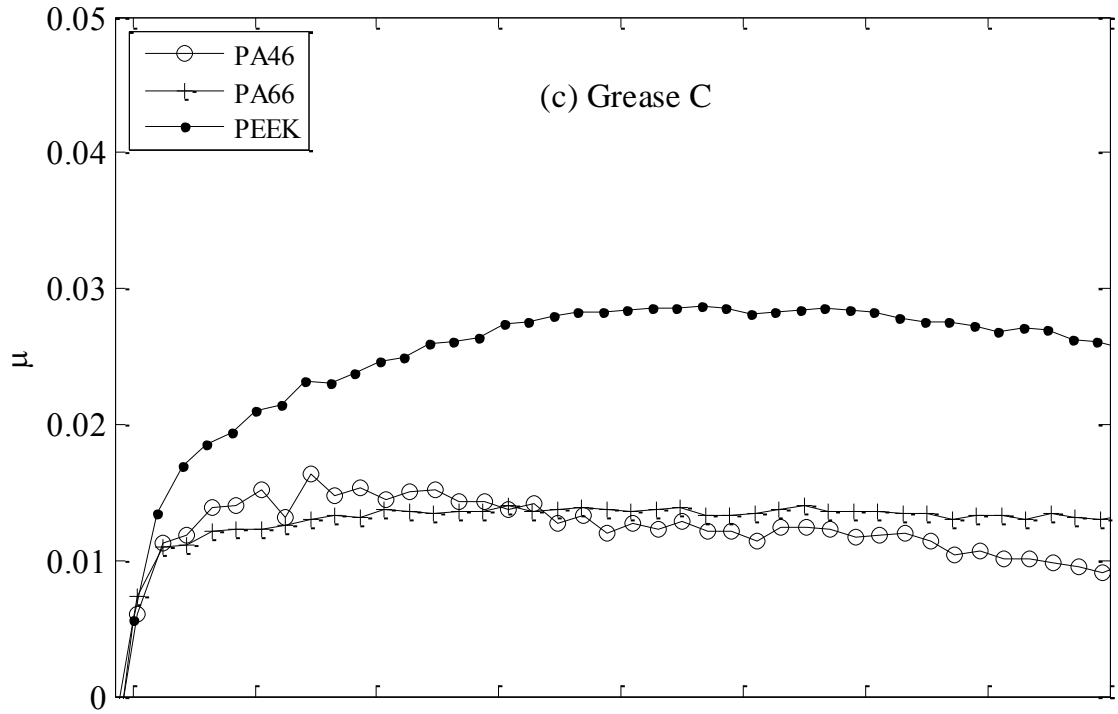


Table 3.1 Measured average friction coefficient $\bar{\mu}$ values for all material-grease pairs tested for $u_r = 5$ m/s and $F_n = 200$ N.

Grease Type	Plastic Type		
	PA46	PA66	PEEK
A	0.035	0.037	0.027
B	0.025	0.035	0.026
C	0.012	0.014	0.027
D	0.016	0.015	0.015

Table 3.2 Measured changes in surface roughnesses during the traction tests.

Plastic Type	Grease Type	Surface roughness Ra [μm]		
		Initial	After Test	% Change
PA46	A	0.78	0.74	-5.1
	B	0.93	0.82	-12.5
	C	0.93	0.70	-25.2
	D	0.97	0.85	-12.7
PA66	A	0.87	0.78	-10.6
	B	0.82	0.74	-10.4
	C	0.85	0.71	-16.4
	D	0.88	0.78	-12.0
PEEK	A	0.48	0.48	-1.3
	B	0.43	0.28	-35.5
	C	0.44	0.37	-17.1
	D	0.46	0.44	-3.9

3.2 Wear Tests

All of the tests were run under the same operating conditions of $F_n = 500\text{N}$, $u_r = 5\text{ m/s}$, and $R = -1.0$. With the three different disk materials (PA46, PA66 and PEEK) and the four types of greases, a total of 12 wear tests were performed as part of this study. Each test was run to a total of 1 million cycles of the disk, which corresponded to a test duration of 817 minutes (13.6 hours). The disks were inspected at 0.2 million cycle (163.4 minute) increments and the surface roughness and profile measurements were made at three equally spaced locations. With the initial, interim and final inspections, each test required about three work days to be completed.

3.2.1 Wear Test Results

Figures 3.5 to 3.16 show the measured wear profiles from all 12 wear tests with different plastic materials and greases. Here, each figure representing a material-grease combination consists of three figures of wear measurements at three circumferential locations that are 120 degrees apart from each other. Each of these sub-figures includes 6 wear traces taken at 0M (initial), 0.2M, 0.4M, 0.6M, 0.8M and 1M (final) cycles of the wear test. The maximum difference between a trace after certain cycles and the initial trace was used as the maximum wear depth at that cycle. Likewise maximum difference between traces for 0 and 1M cycles represented the maximum final wear depth.

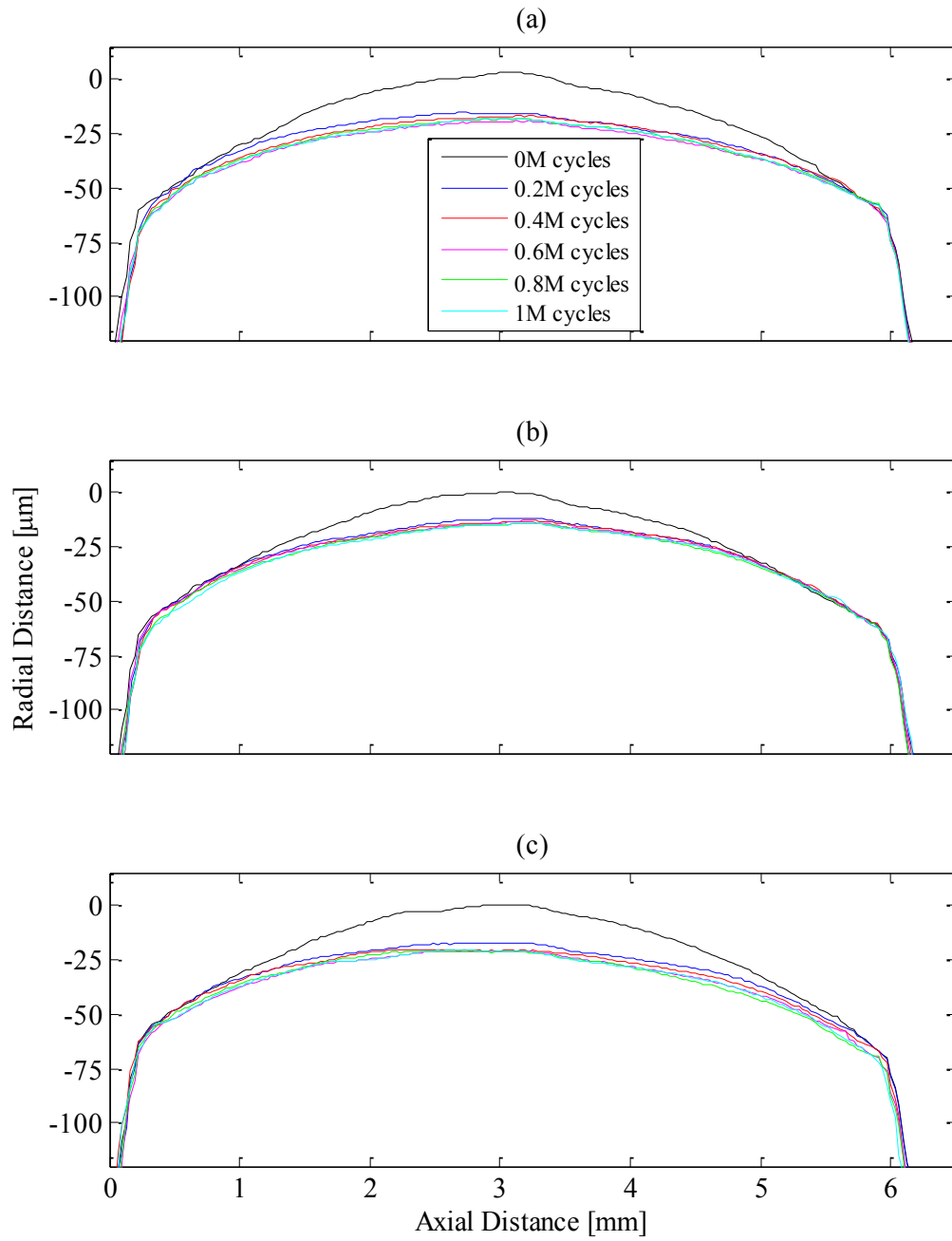


Figure 3.5 Profile measurements for PA46 with Grease A at three measurement locations for $u_r = 5$ m/s, $F_n = 500\text{N}$, and $R = -1$.

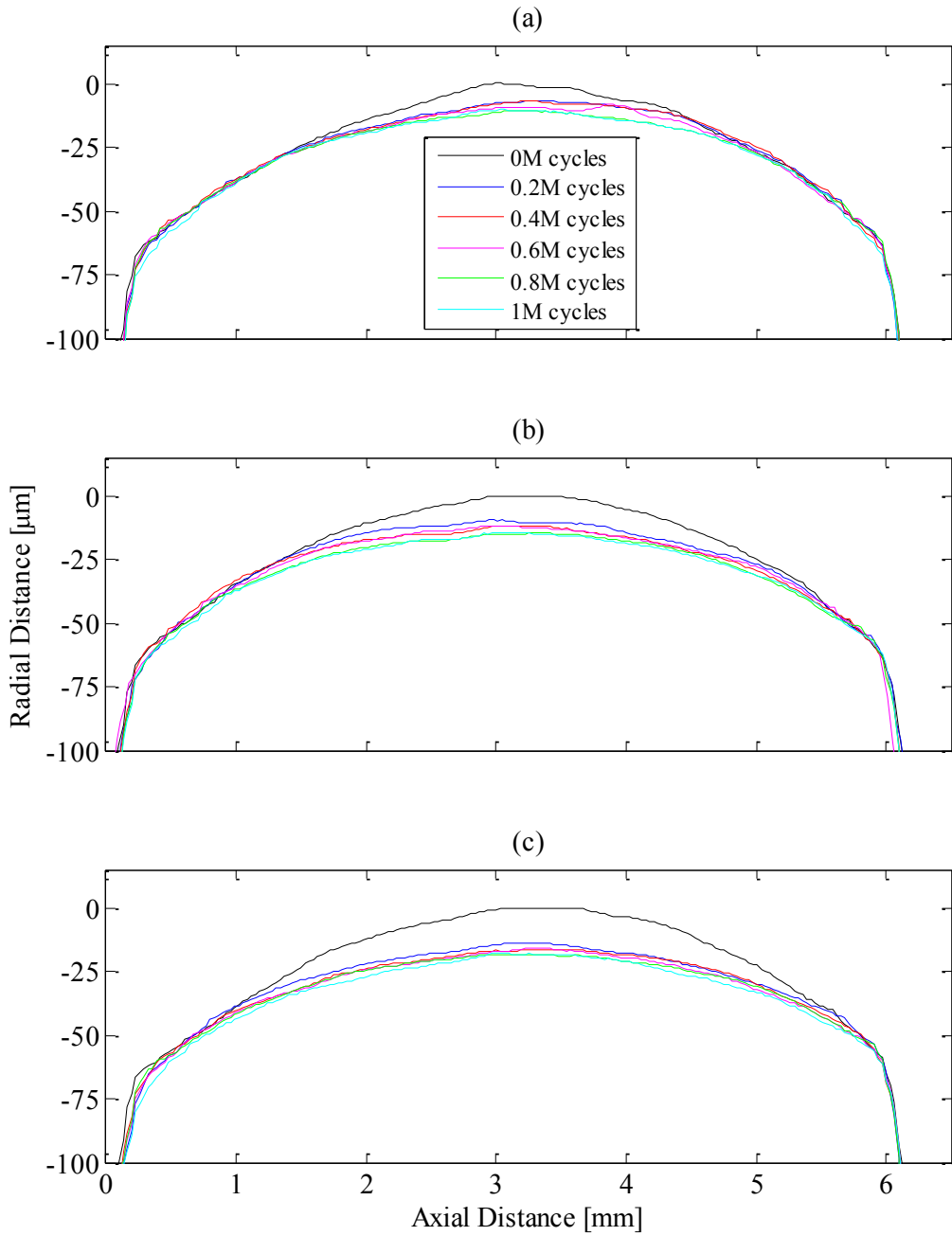


Figure 3.6 Profile measurements for PA46 with Grease B at three measurement locations for $u_r = 5$ m/s, $F_n = 500$ N, and $R = -1$.

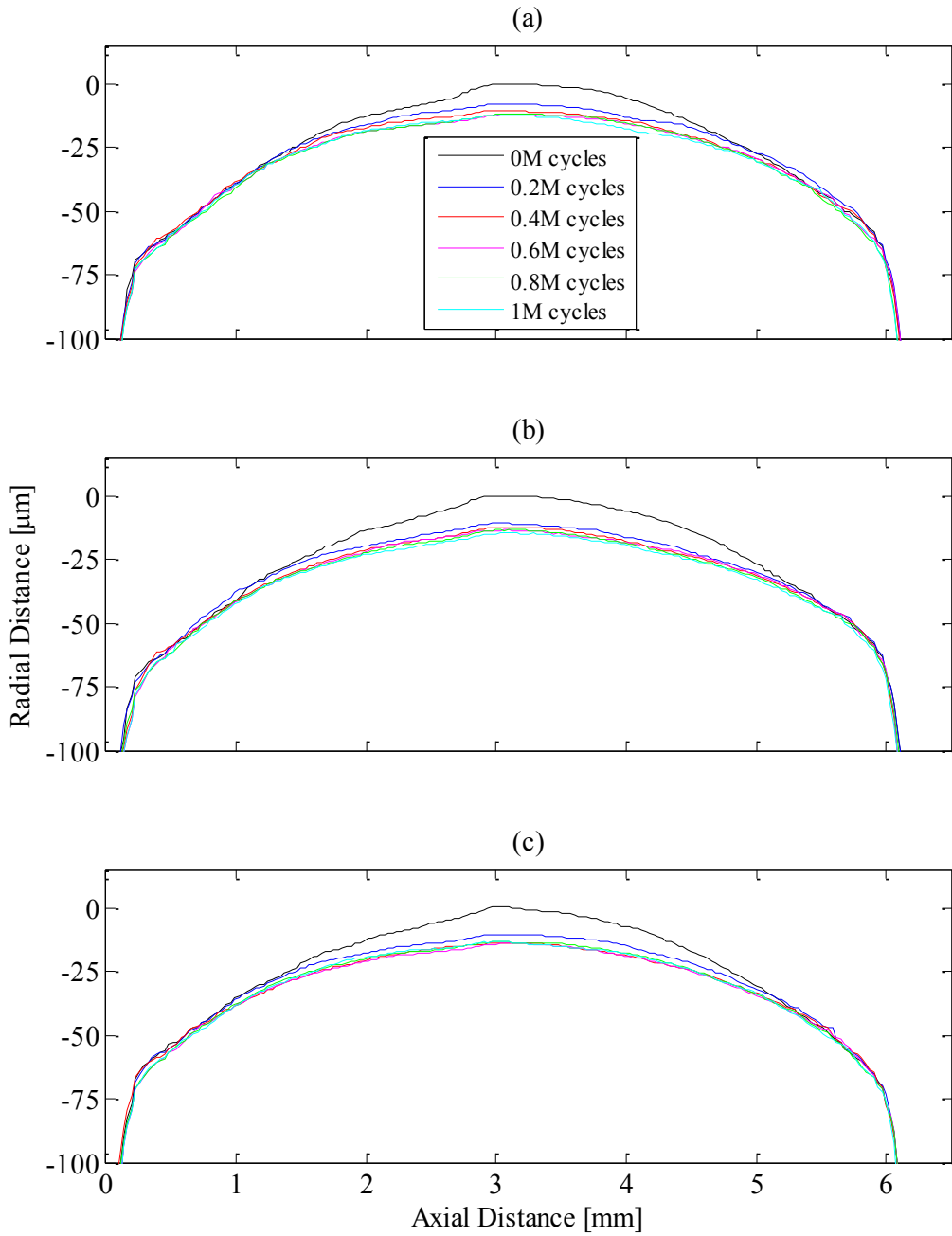


Figure 3.7 Profile measurements for PA46 with Grease C at three measurement locations for $u_r = 5$ m/s, $F_n = 500$ N, and $R = -1$.

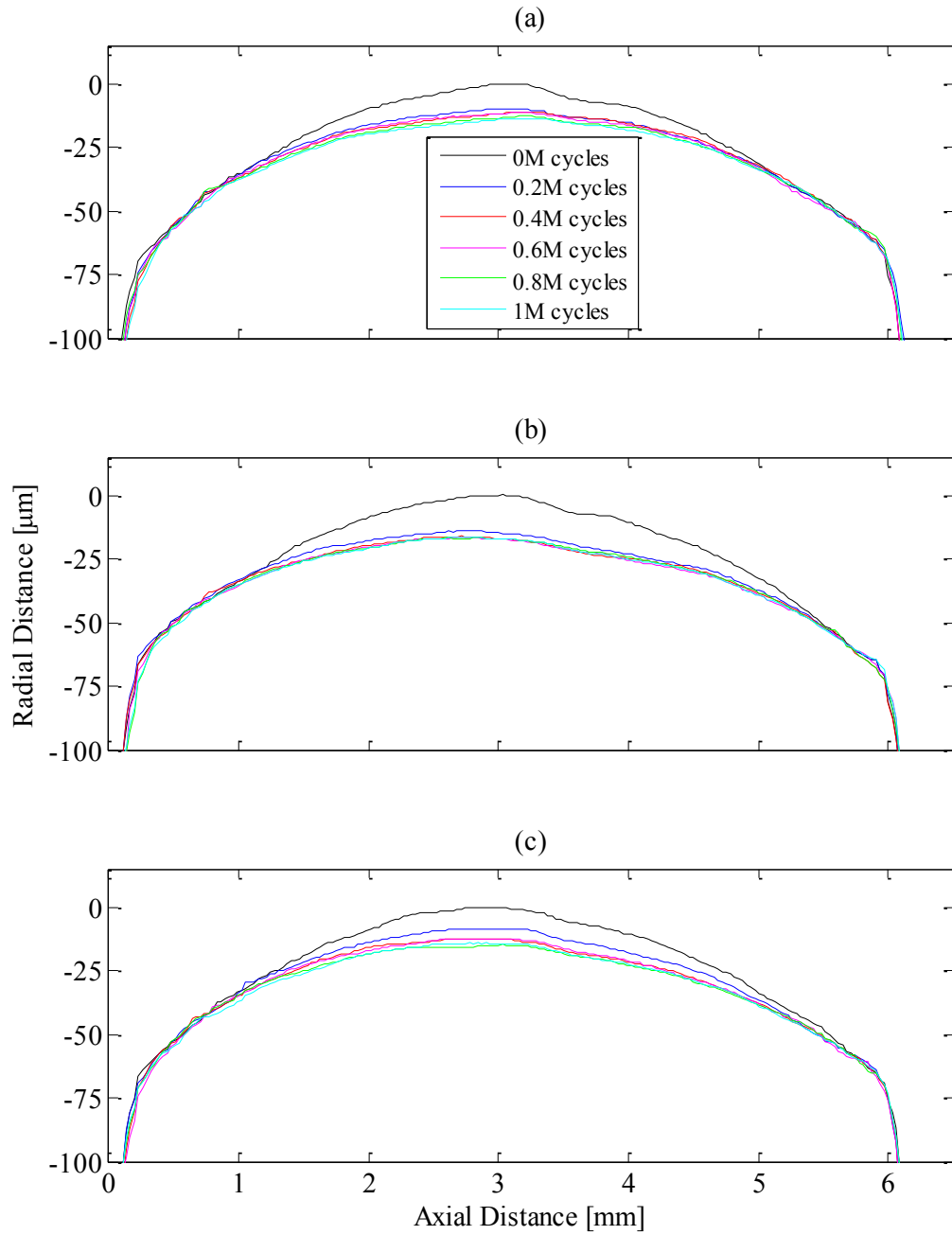


Figure 3.8 Profile measurements for PA46 with Grease D at three measurement locations for $u_r = 5$ m/s, $F_n = 500\text{N}$, and $R = -1$.

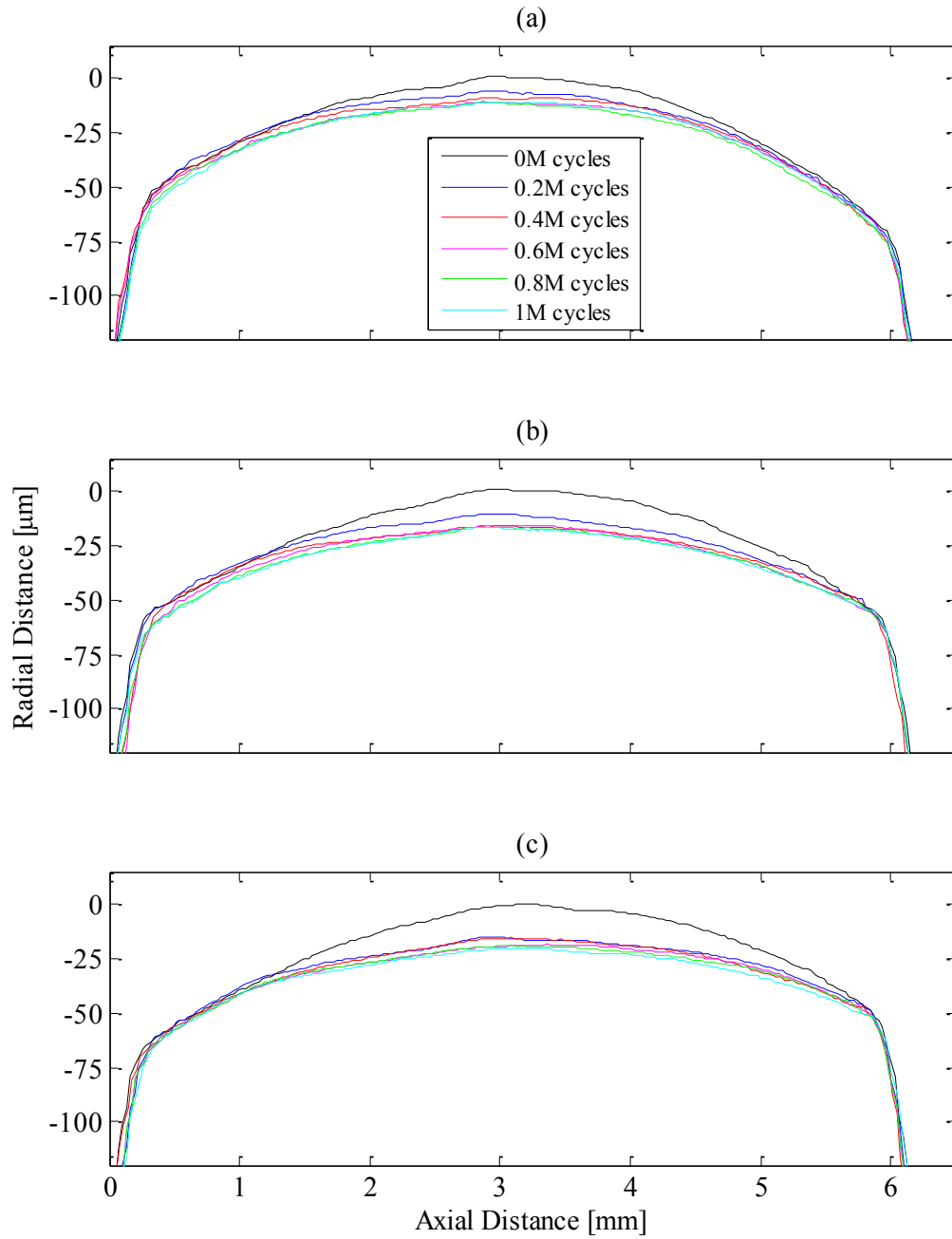


Figure 3.9 Profile measurements for PA66 with Grease A at three measurement locations for $u_r = 5$ m/s, $F_n = 500\text{N}$, and $R = -1$.

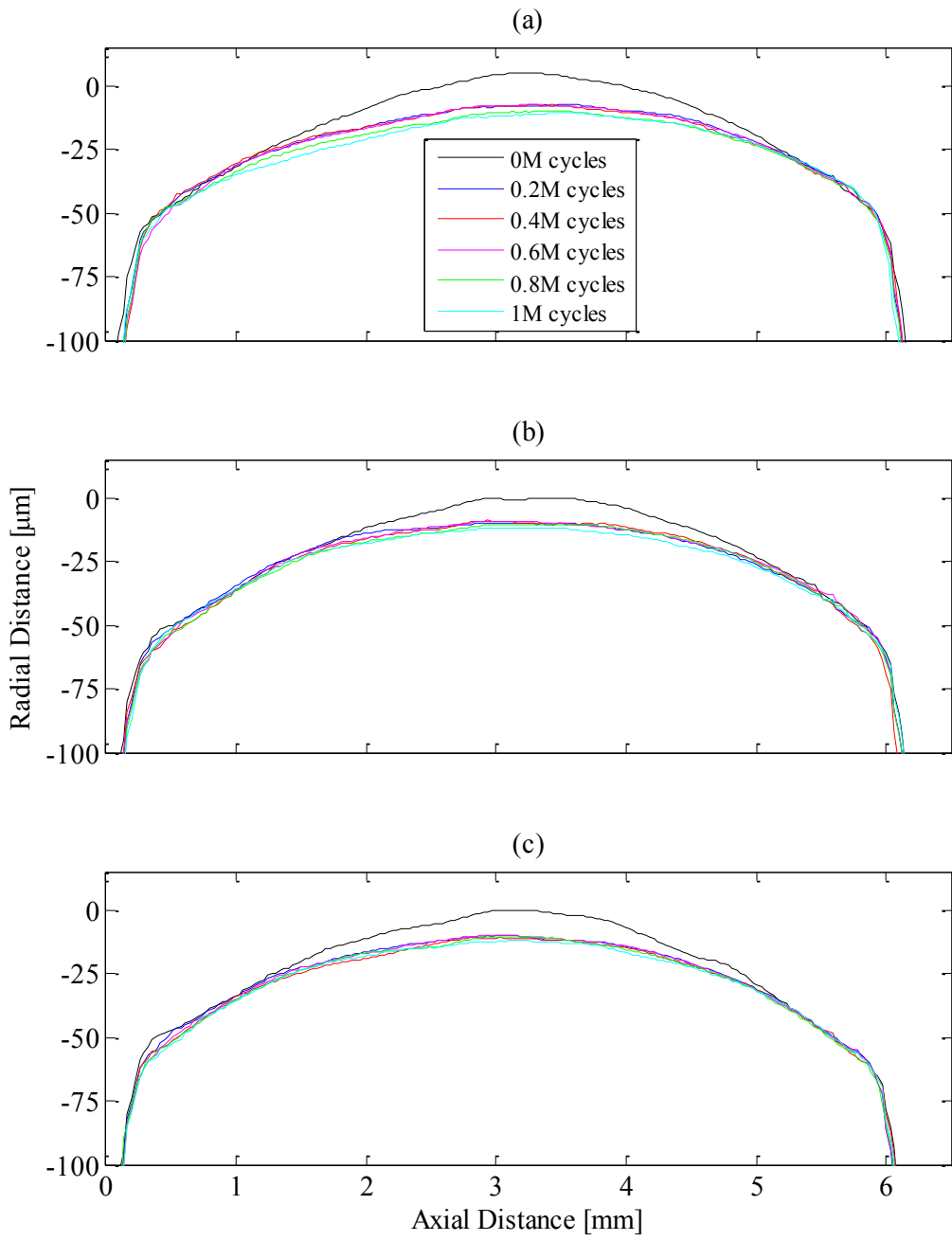


Figure 3.10 Profile measurements for PA66 with Grease B at three measurement locations for $u_r = 5$ m/s, $F_n = 500$ N, and $R = -1$.

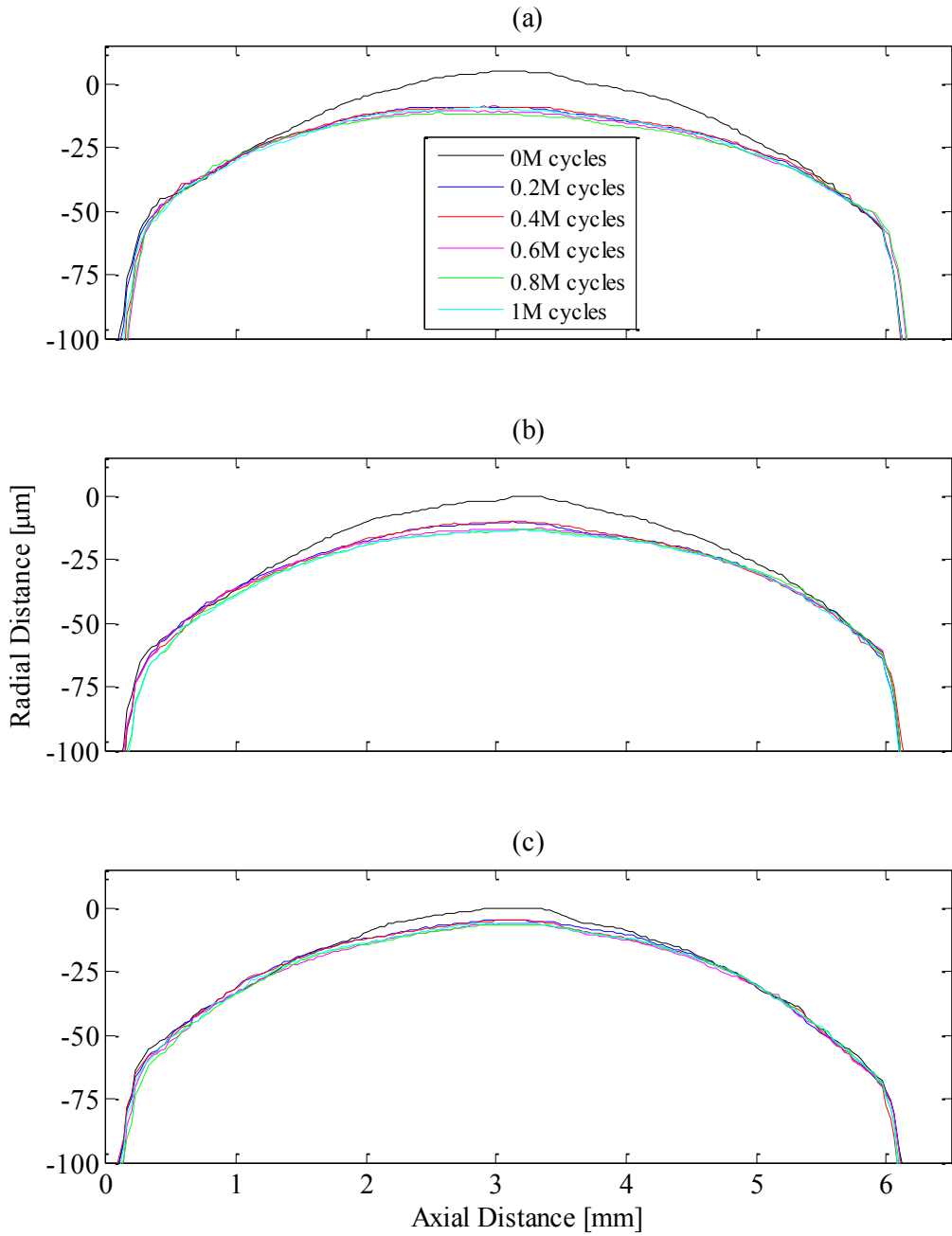


Figure 3.11 Profile measurements for PA66 with Grease C at three measurement locations for $u_r = 5$ m/s, $F_n = 500$ N, and $R = -1$.

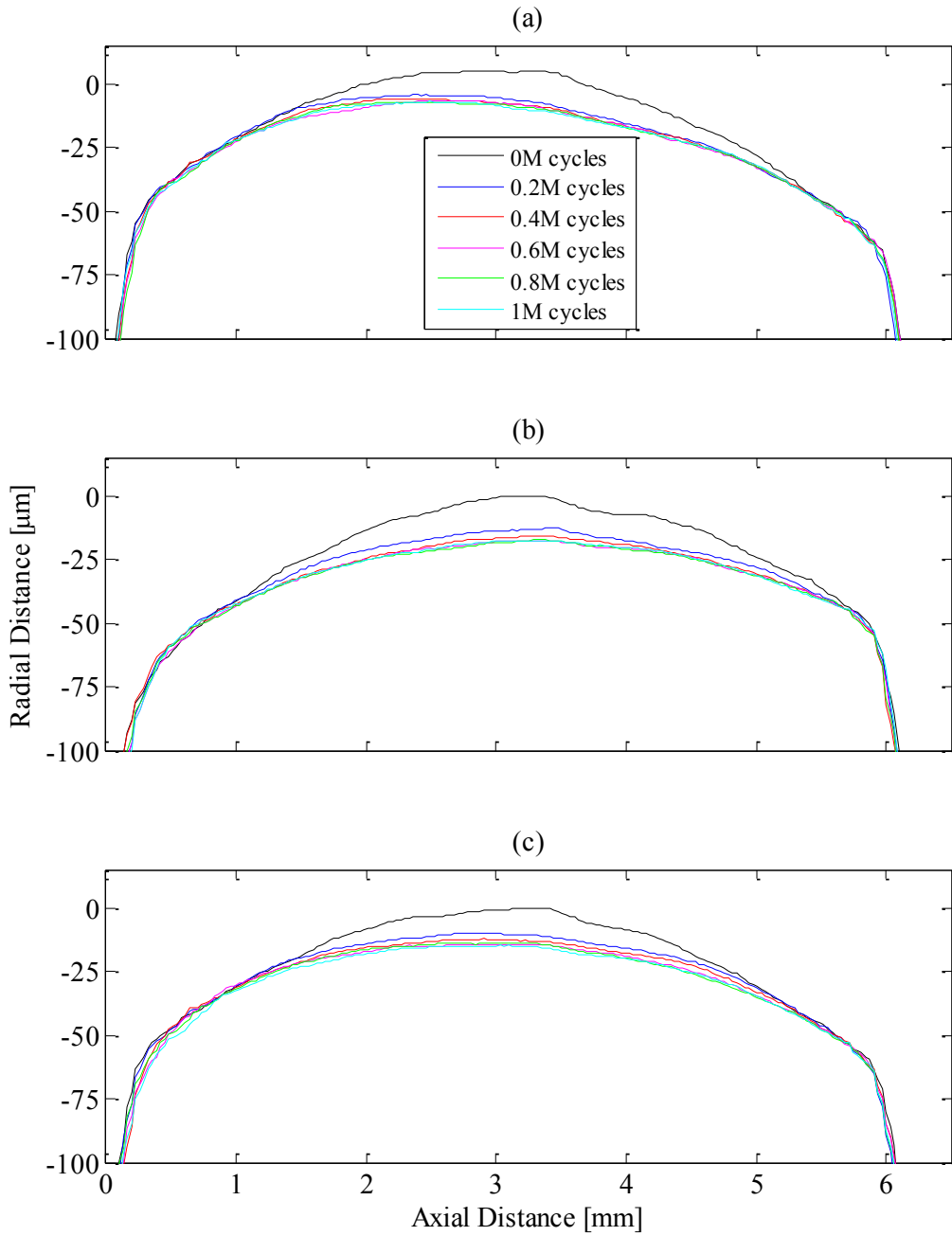


Figure 3.12 Profile measurements for PA66 with Grease D at three measurement locations for $u_r = 5$ m/s, $F_n = 500$ N, and $R = -1$.

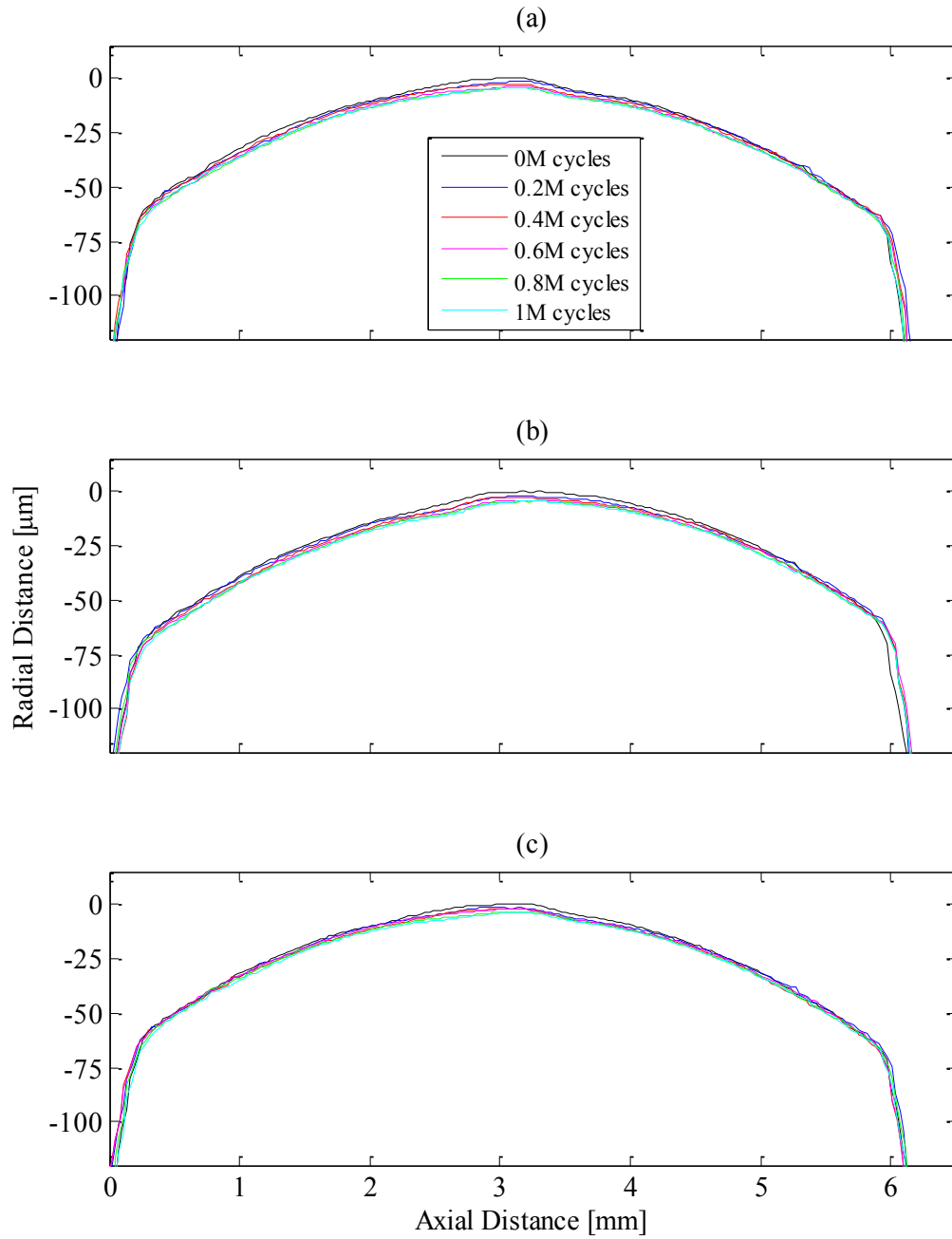


Figure 3.13 Profile measurements for PEEK with Grease A at three measurement locations for $u_r = 5$ m/s, $F_n = 500$ N, and $R = -1$.

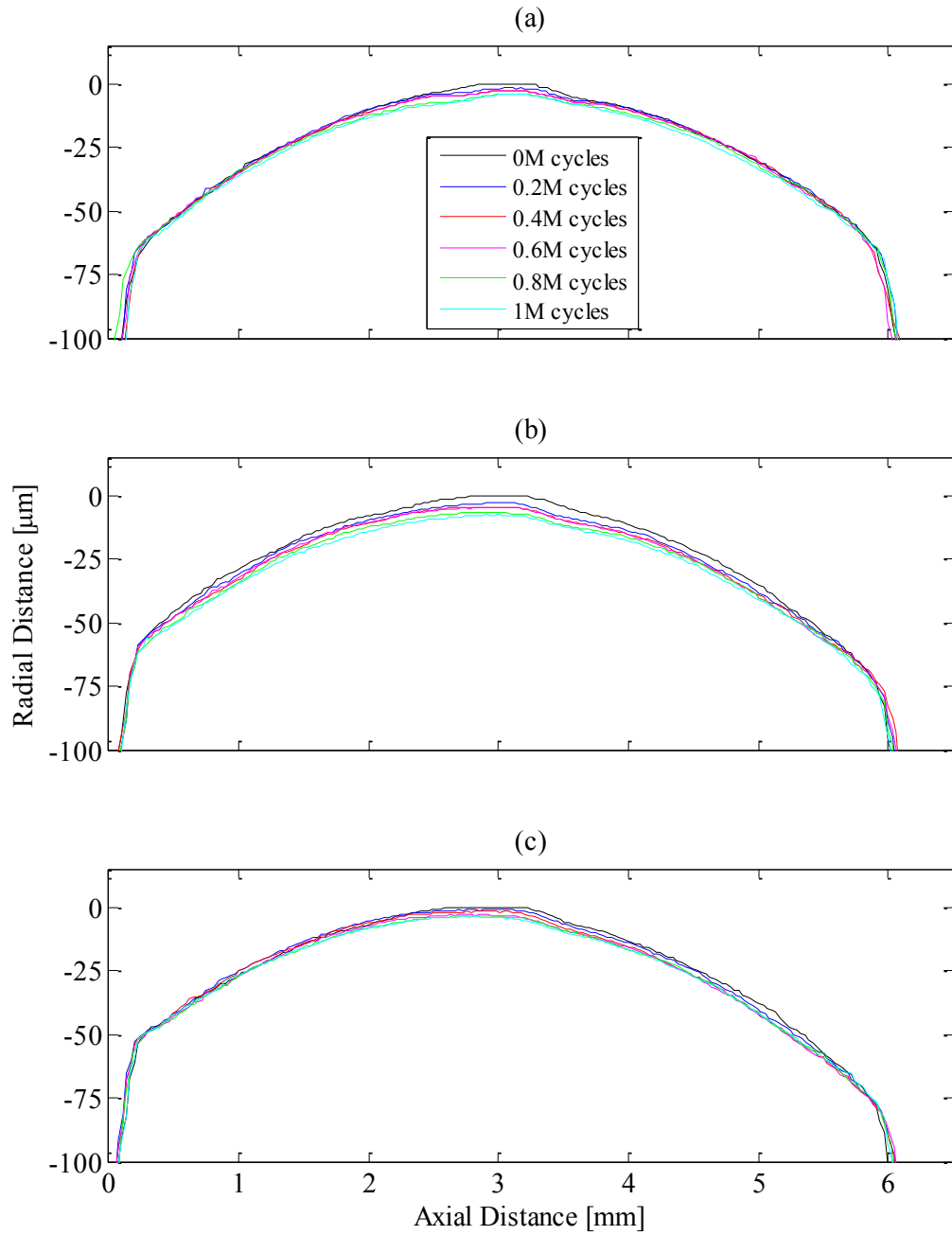


Figure 3.14 Profile measurements for PEEK with Grease B at three measurement locations for $u_r = 5$ m/s, $F_n = 500$ N, and $R = -1$.

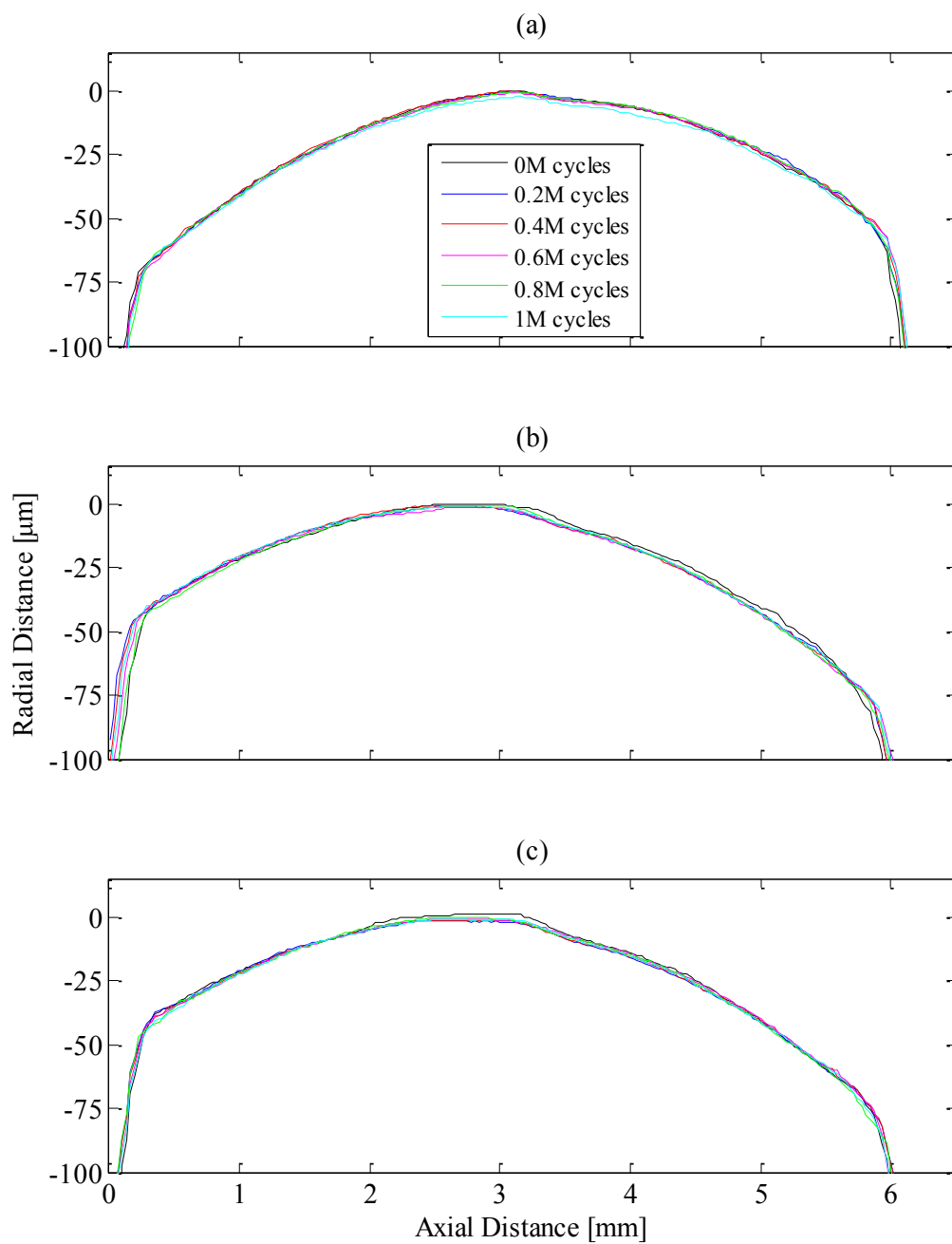


Figure 3.15 Profile measurements for PEEK with Grease C at three measurement locations for $u_r = 5$ m/s, $F_n = 500$ N, and $R = -1$.

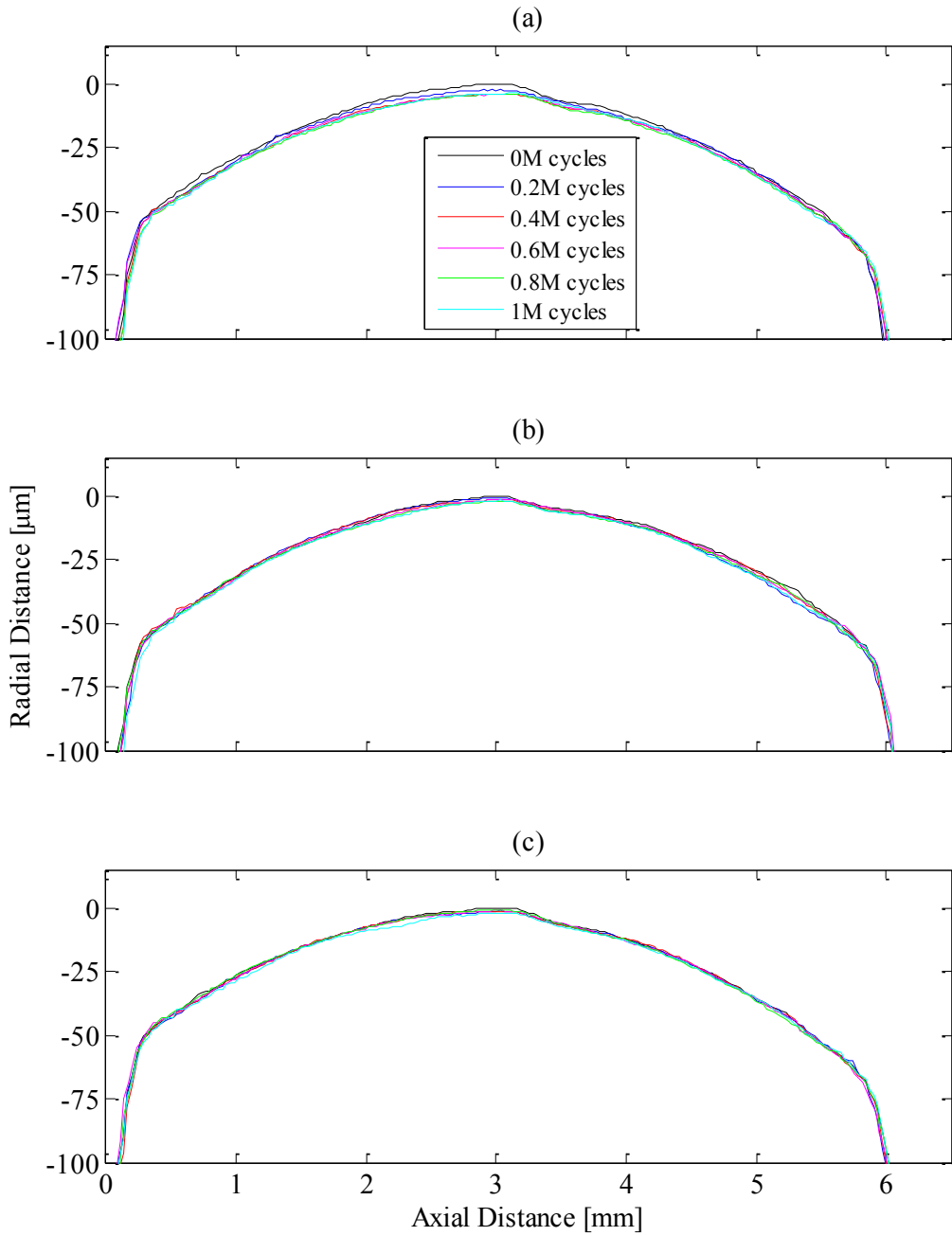


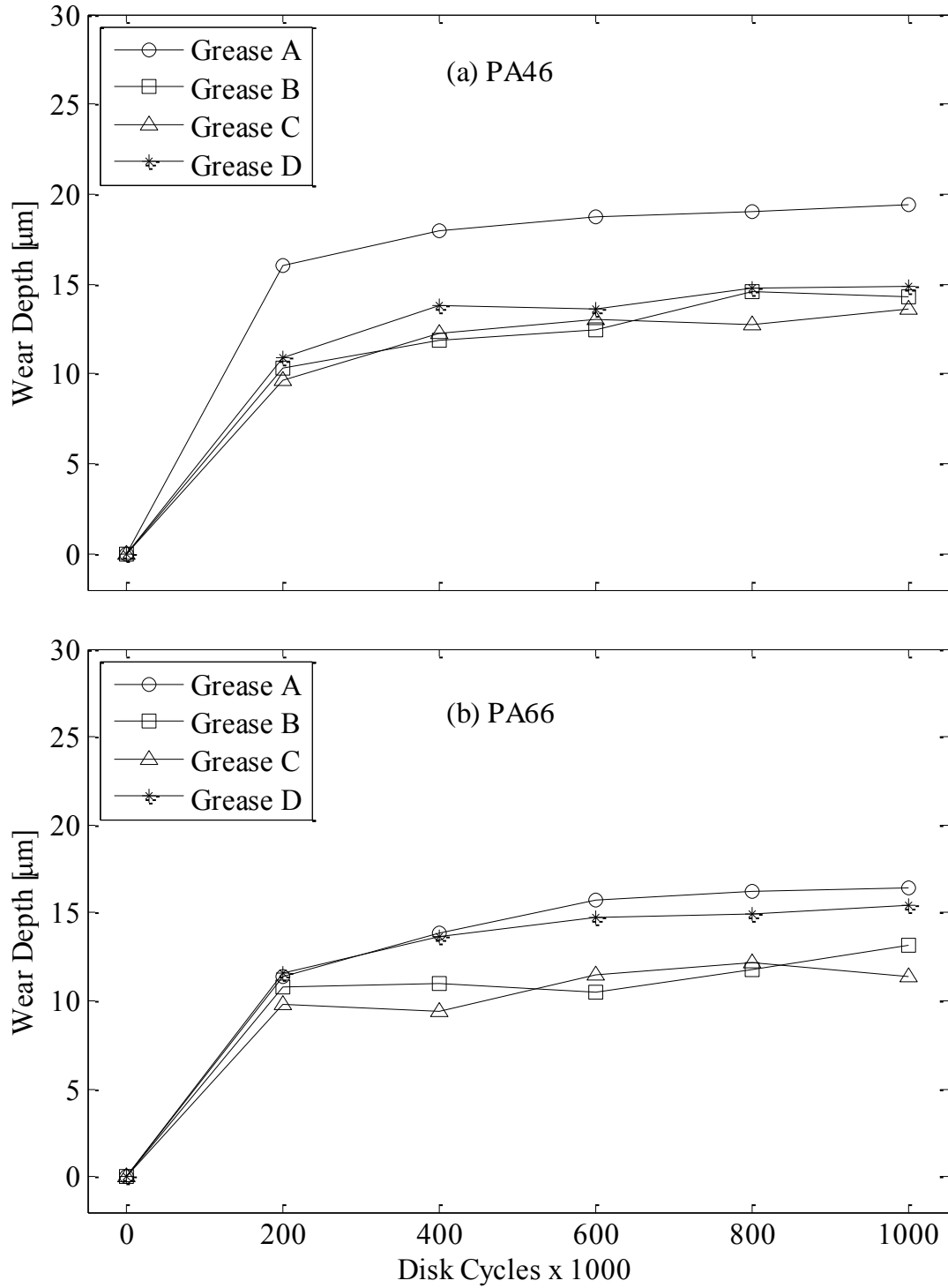
Figure 3.16 Profile measurements for PEEK with Grease D at three measurement locations for $u_r = 5$ m/s, $F_n = 500$ N, and $R = -1$.

It is noted in Figures 3.5 to 3.16 that the wear depths are quite consistent amongst the three circumferential locations, indicating a uniform and consistent wear track along the circumference of each disk. It is also noted that the wear rate (depth/cycles) is not constant throughout a test. The maximum gap is between the 0 and 0.2M traces indicating that wear rate is high initially. In order to quantify the measurement of wear depth in Figures 3.5 to 3.16 and demonstrate this apparent change in wear rates, Figure 3.17 is presented showing the maximum wear depths as a function of wear cycles, showing comparisons for each material type separately. The same data is presented in Figure 3.18 for each grease type separately. Furthermore, Table 3.3 summarized the final maximum wear depths from all 12 tests. In view of Figures 3.17, 3.18, and Table 3.3, the following observations can be made in regards to wear performance of greases and plastic materials used in this study:

- Overall, the combination of PEEK with Grease D performed the best with a wear depth of only 2.1 μm after 1M cycles.
- The worst performing combination was PA46 and Grease A with a maximum wear depth of 19.4 μm , showing a difference of 17.3 μm between the best and worst performing material-grease combinations.
- PEEK showed the least amount of wear regardless of the choice of grease with maximum wear depths of 4.2 μm , 5.6 μm , 2.4 μm , and 2.1 μm with Greases A-D respectively.
- PA46 showed the largest amount of wear with Greases A-C, while PA66 showed the largest amount of wear when used with Grease D.

- It was observed that Grease C is the best choice for PA46 and PA66 while Grease D is the best choice for PEEK. However, Grease C could also be used effectively with PEEK since the wear depth of the PEEK-Grease C combination is only 0.3 μm greater than the PEEK-Grease D combination.
- All of the material-grease combinations showed a large initial wear rate from 0 to 0.2M cycles and a smaller wear rate for the duration of the test due to widening contact track which reduced the contact stress, thus reducing wear.

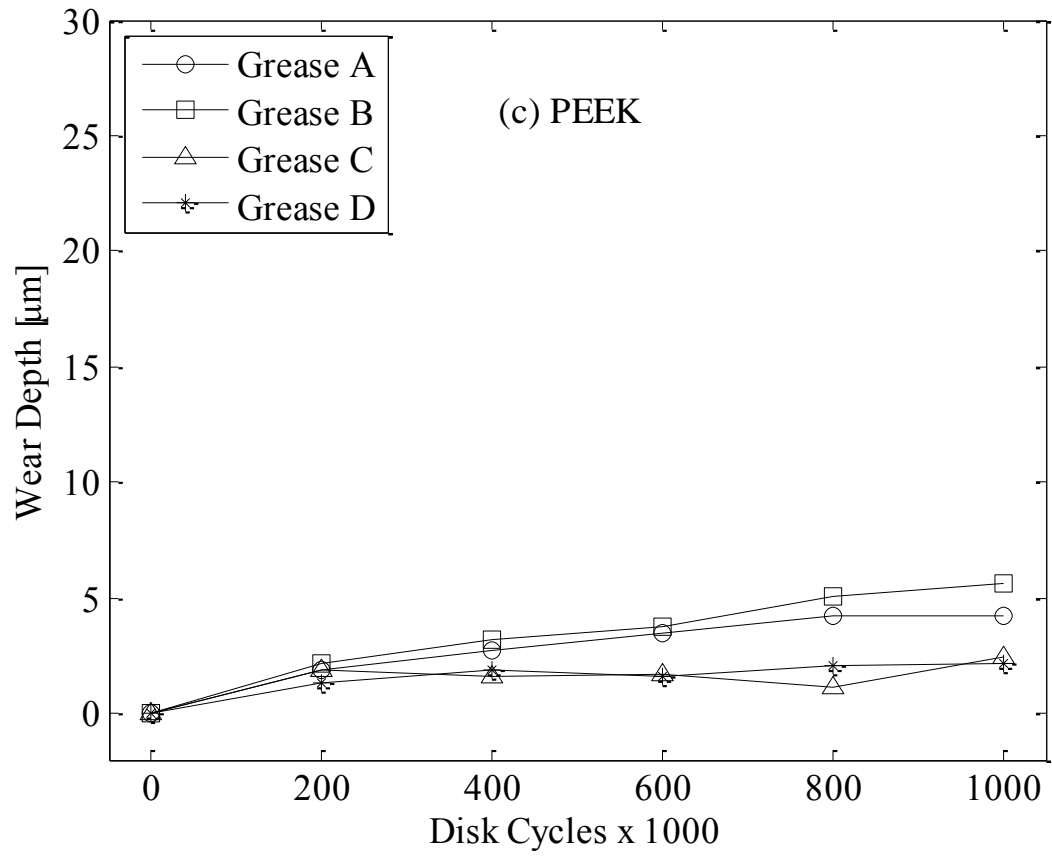
In order to complement Figure 3.17 and 3.18, corresponding surface roughness changes ($\Delta R_a = R_a - R_{a,initial}$) are plotted in Figures 3.19 and 3.20 respectively. In addition, the initial and final R_a values are listed in Table 3.4 to complement Table 3.3. From Figures 3.19 and 3.20, it is observed that the surface roughnesses experience their greatest reduction during the first stage of wear tests from 0 to 0.2M cycles. At the end of a 1M cycle wear test, the specimens typically become smoother with reductions in R_a from about 0 to 0.35 μm . Both PA46 and PA66 disks follow similar smoothing trends with cycles regardless of grease type while PEEK disks with greases A, C and D do not exhibit tangible reductions in R_a with cycles.

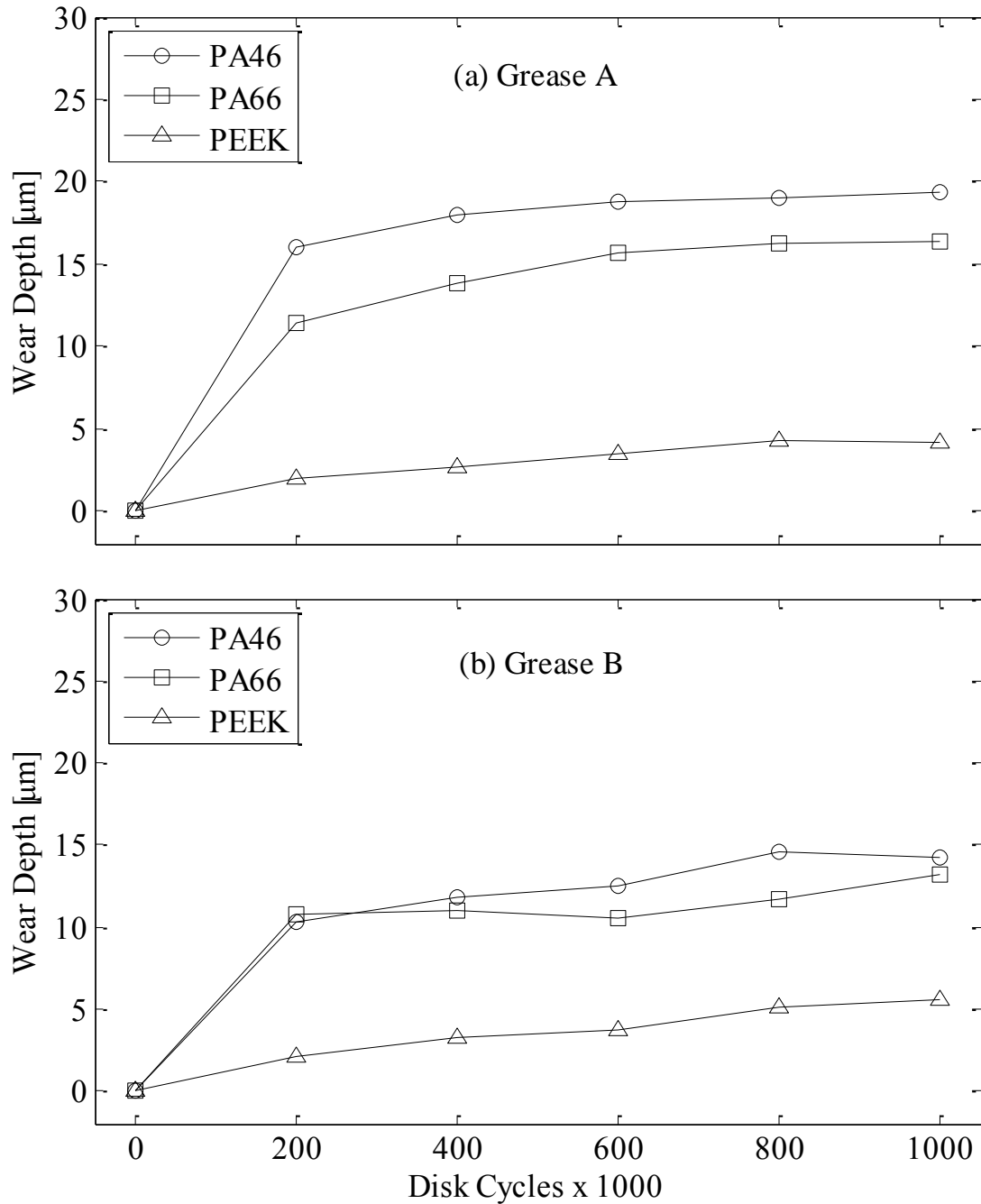


Continued.

Figure 3.17 Variation of measured average wear depth with loading cycles at $u_r = 5$ m/s, $F_n = 500$ N, and $R = -1$ for (a) PA46, (b) PA66, and (c) PEEK disks.

Figure 3.17 Continued.

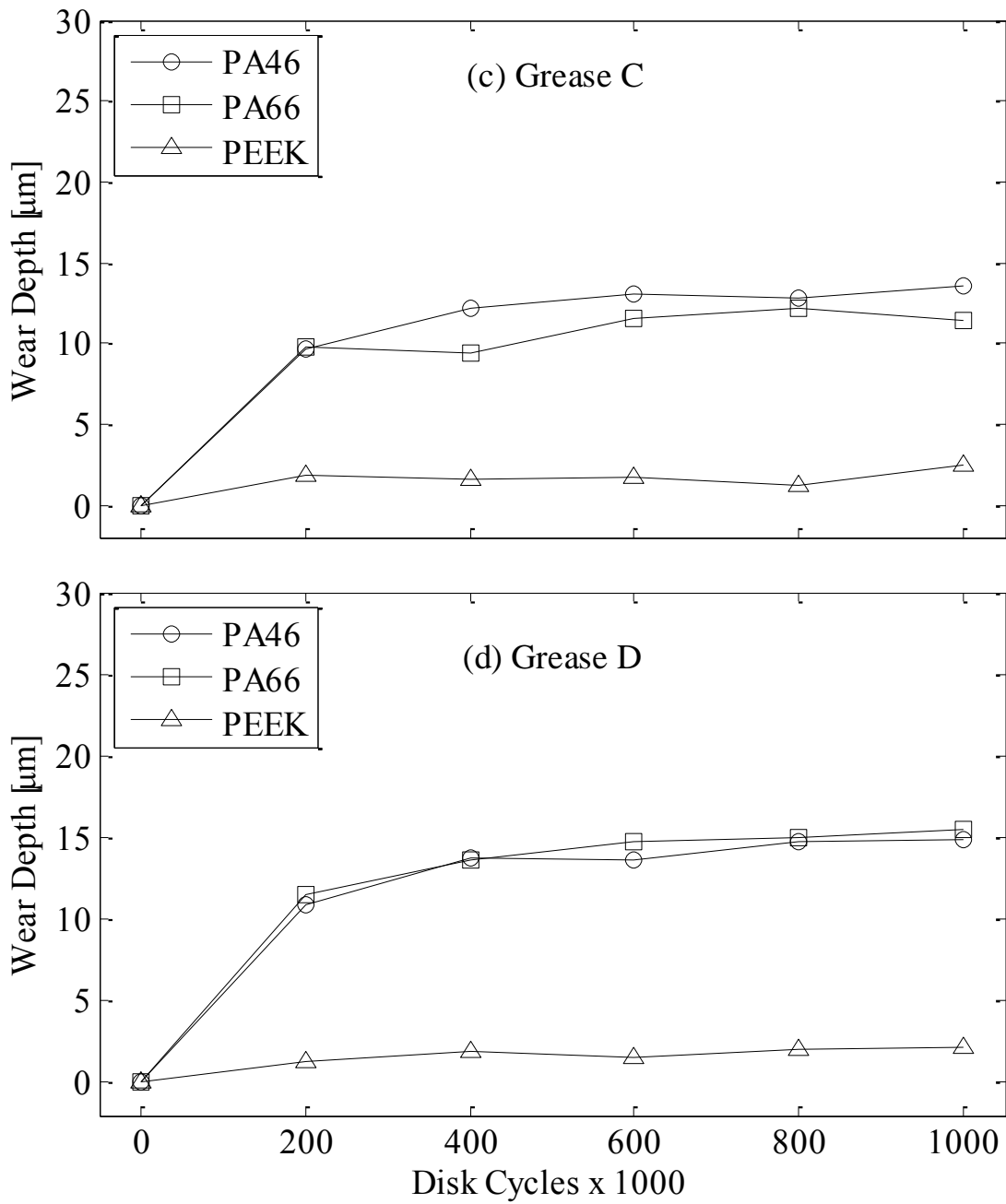


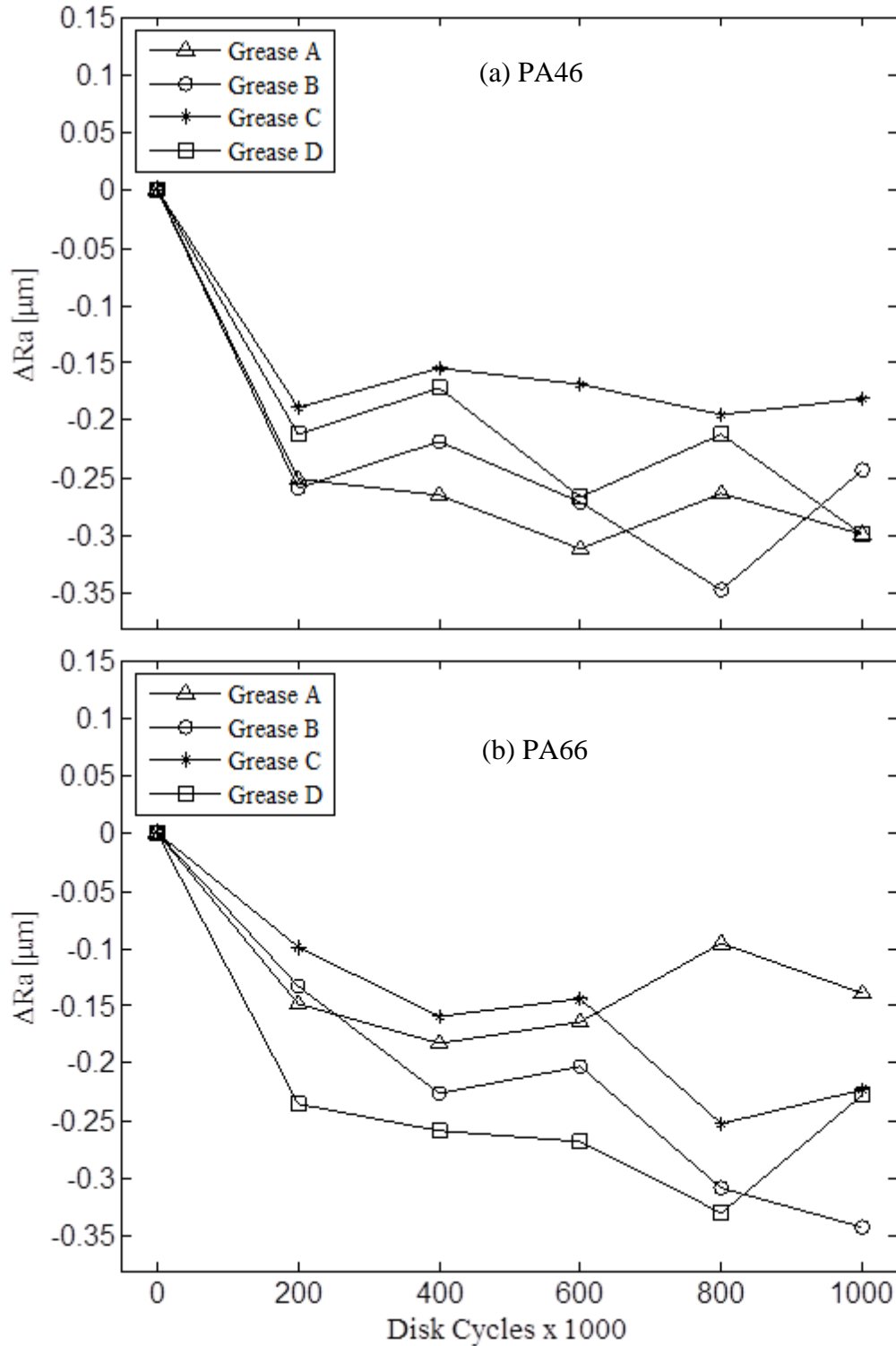


Continued.

Figure 3.18 Variation of measured average wear depth with loading cycles at $u_r = 5$ m/s, $F_n = 500$ N, and $R = -1$ for (a) Grease A, (b) Grease B, (c) Grease C and (d) Grease D.

Figure 3.18 Continued.

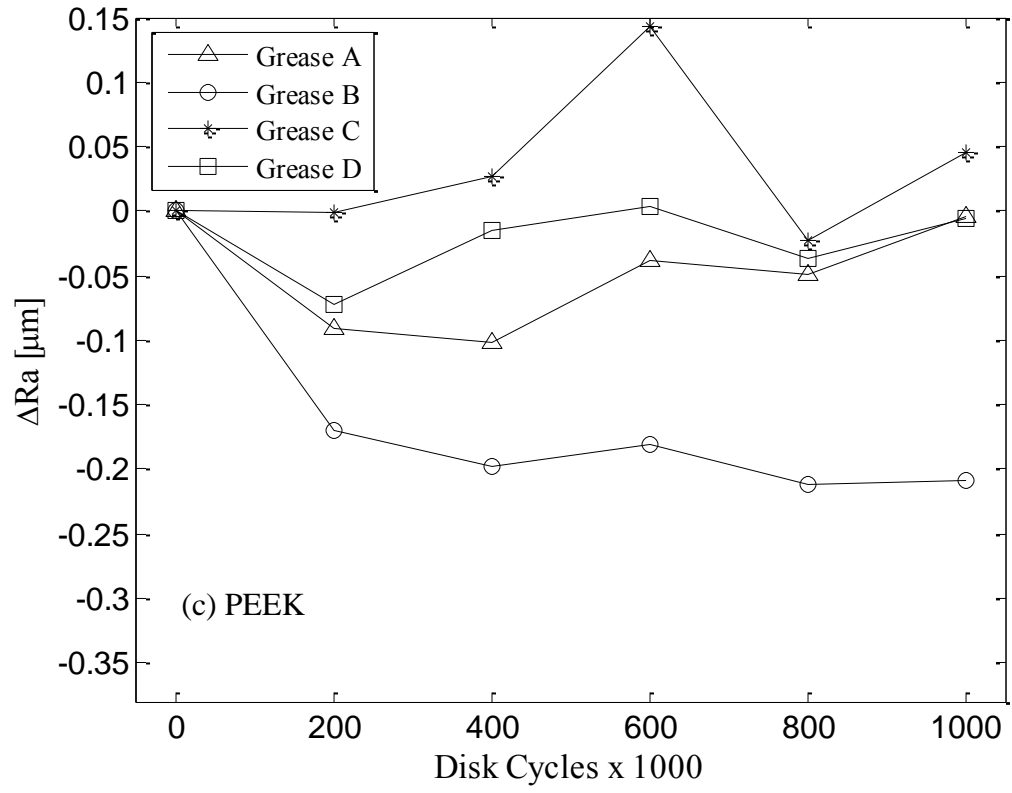


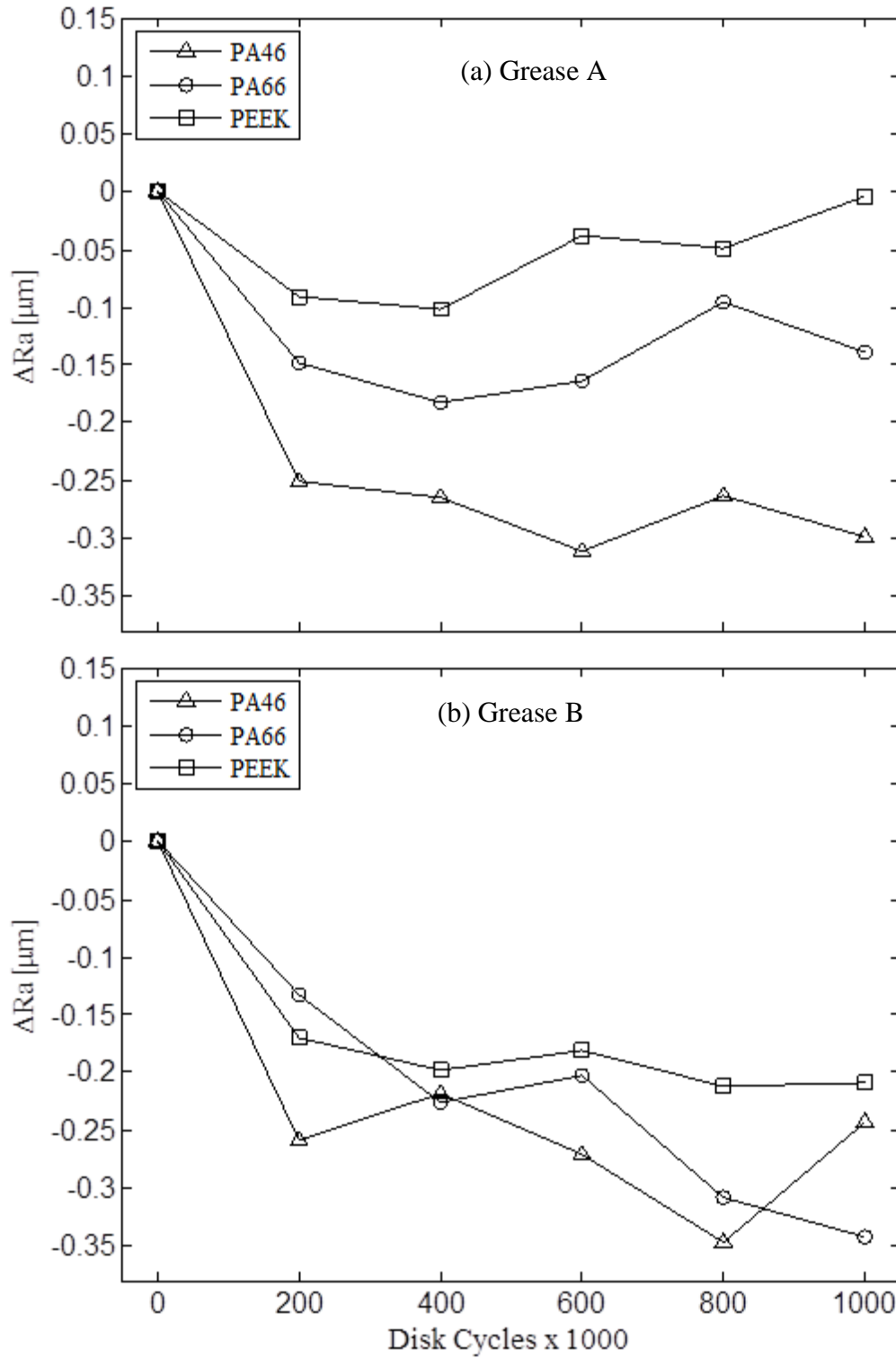


Continued.

Figure 3.19 Changes in R_a values of surfaces with loading cycles for (a) PA46 disks, (b) PA66 disks and (c) PEEK disks.

Figure 3.19 Continued.

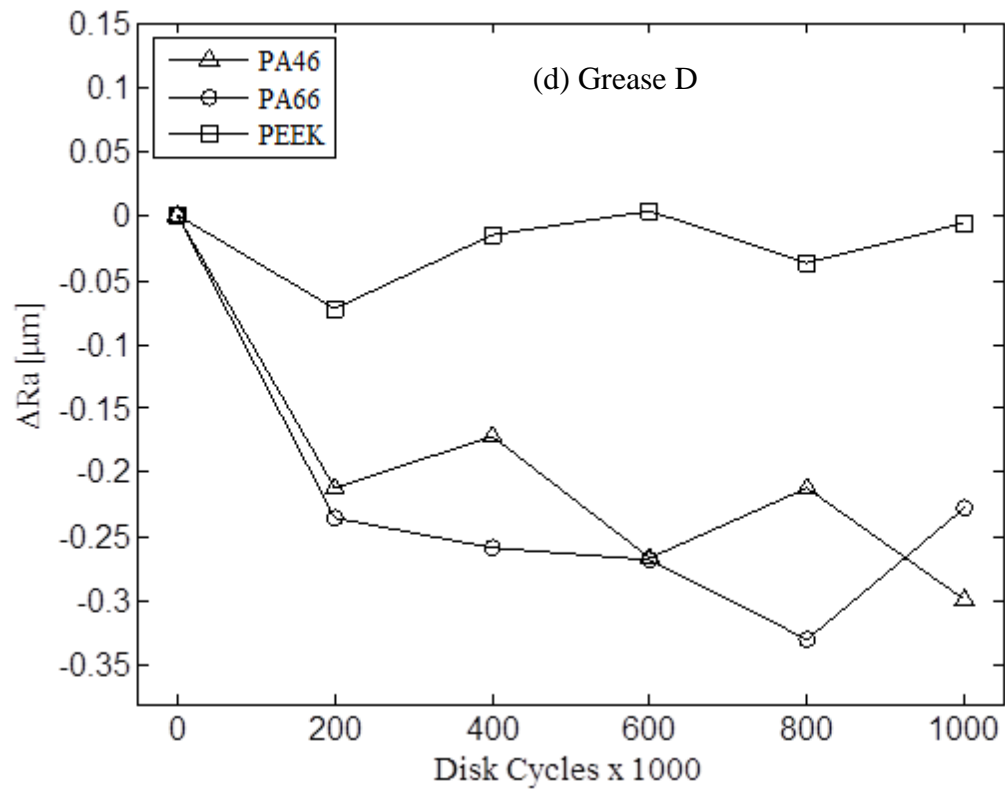
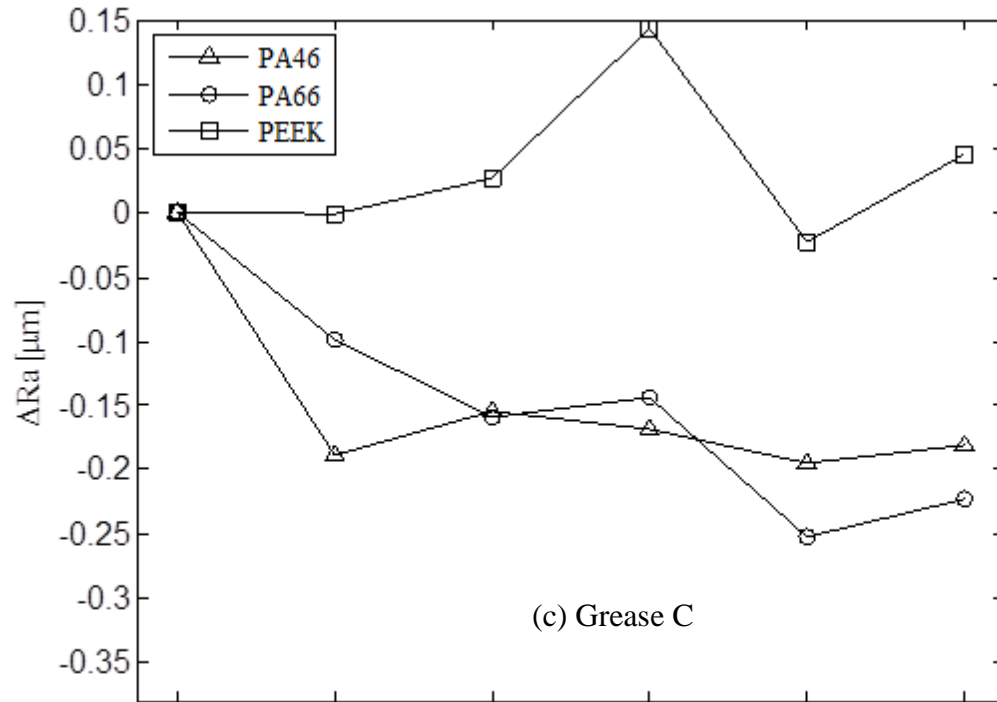




Continued.

Figure 3.20 Changes in R_a values of surfaces with loading cycles for (a) Grease A, (b) Grease B, (b) Grease C and (c) Grease D.

Figure 3.20 Continued.



3.2.2 Steel Roller Results

As all tests were performed with a plastic disk mating with a case-hardened steel roller, the roller was not expected to experience any sizable wear accumulation or changes to its surface roughness amplitudes. Figure 3.21 shows the wear profiles of the steel roller at three circumferential positions before and after the entire wear test to indicate that no detectible wear was accumulated during the wear tests. Likewise, Figure 3.22 shows the R_a values of the steel roller after completion of a set of wear tests with each grease type. As seen here, the R_a value of the roller was $0.14\ \mu\text{m}$ initially, which remain within $\pm 0.1\ \mu\text{m}$ of it through the entirety of these wear tests indicating that steel roller played little or no role in the wear behavior observed for different plastic materials with different greases.

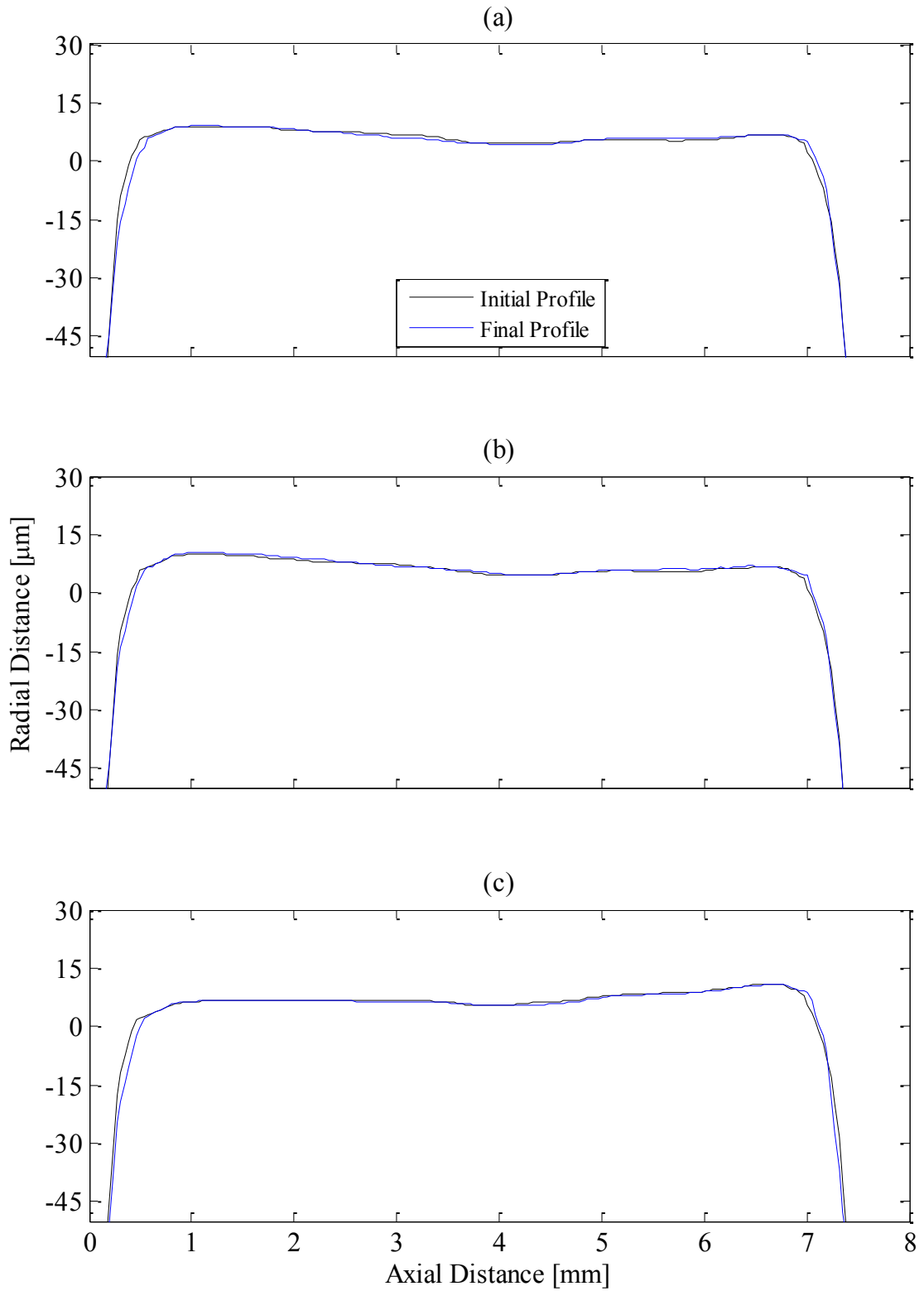


Figure 3.21 Comparison of steel roller profiles at three locations before and after the entire wear program.

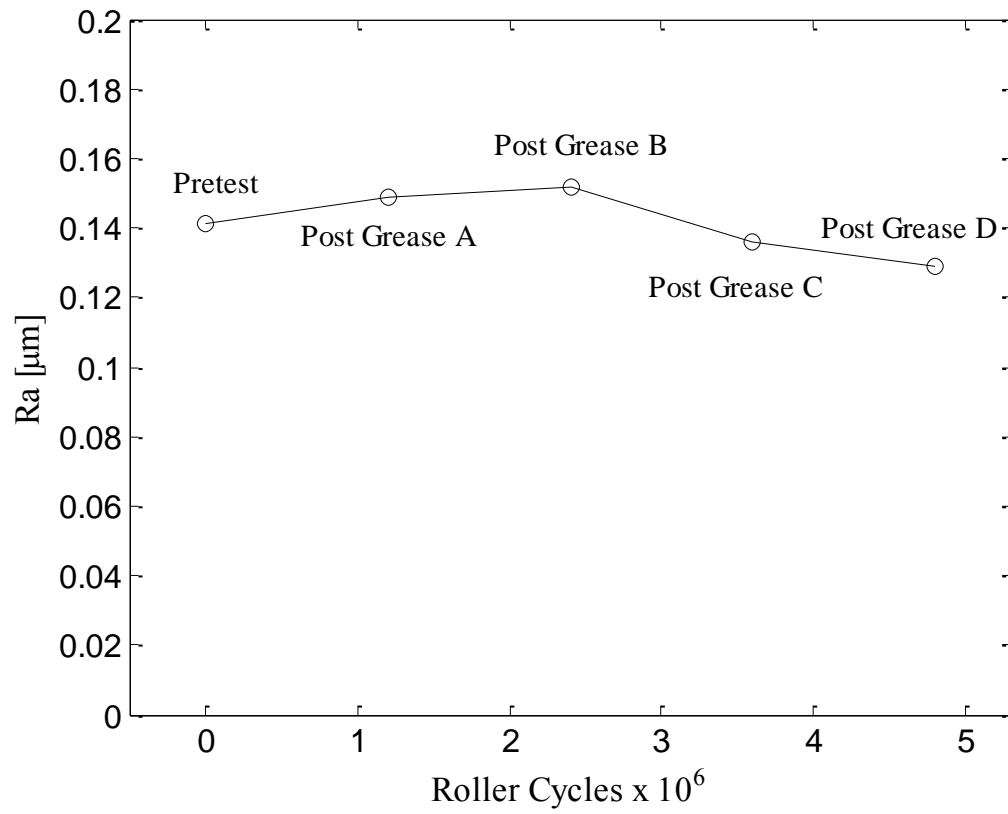


Figure 3.22 Measured variation of the initial R_a value of the steel roller after wear tests using different greases.

Table 3.3 Measured maximum final wear depth values (in μm) for all material-grease pairs tested for $u_r = 5$ m/s, $F_n = 500$ N and $R = -1.0$.

Grease Type	Plastic Type		
	PA46	PA66	PEEK
A	19.4	16.4	4.2
B	14.3	13.2	5.6
C	13.6	11.4	2.4
D	14.8	15.5	2.1

Table 3.4 Summary of surface roughness measurements during wear test results.

Plastic Type	Grease Type	Surface roughness Ra [μm]		
		Initial	After Test	% Change
PA46	A	0.83	0.53	-35.9
	B	0.89	0.65	-27.3
	C	0.79	0.61	.23.1
	D	0.88	0.58	-33.9
PA66	A	0.85	0.72	-16.3
	B	0.83	0.48	-41.3
	C	0.82	0.60	-27.0
	D	0.84	0.61	-27.3
PEEK	A	0.43	0.42	-0.9
	B	0.48	0.27	-43.4
	C	0.43	0.47	10.8
	D	0.40	0.39	-1.8

CHAPTER 4

CONCLUSIONS

4.1 Summary

In this study, a family of experimental evaluations was conducted to rank order combinations of plastics and greases for their suitability for automotive auxiliary drive applications in terms of their friction and wear performances. The tests included three common plastic materials (PA46 with 30% glass fiber filler, PA66 with 30% glass fiber filler, and PEEK with 30% carbon fiber filler) and four different greases (Greases A to D). Plastic disks were procured and mated with a steel roller using a twin-disk test machine that generates a combined rolling and sliding contact condition as in gears.

Friction tests were conducted to measure the friction coefficient of each plastic-grease combination within a range of slide-to-roll ratios. Wear tests were also conducted for all twelve material-grease combinations with each test consisting of one million loading cycles of each plastic disk. A coordinate measurement machine and a surface roughness profiler were used to assess the wear outcome of each combination. The

friction and wear results were presented in forms to allow direct comparisons in terms of viability of each combination.

4.2 Conclusions

Based on the results presented in Chapter 3, the following general conclusions can be made in terms of the test methodology devised and the materials and greases evaluated:

- The twin-disk test methodology devised in this study was found to be suitable in evaluating traction and wear performance of different plastic materials and greases in a repeatable, accelerated, and cost-effective manner.
- The best performing plastic-grease combination overall was PEEK with Grease D. This combination had the best wear performance with a maximum wear depth of only 2.1 μm after 1M cycles along with the third lowest average friction coefficient of $\bar{\mu} = 0.015$.
- Since PEEK is significantly more expensive and more difficult to machine than PA46 and PA66, a PA product may be chosen for applications if wear is not a primary concern. If PA46 is chosen, it should be used with Grease C as PA46 has the lowest $\bar{\mu}$ and least amount of wear with Grease C as the lubricant. The same behavior was observed for the PA66-Grease C combination based on both maximum wear depth and average sliding friction coefficient.

- Overall, Greases A and B performed poorly for plastic-steel contact as the friction coefficient and wear performances were consistently the worst regardless of the plastic material involved.
- The worst performing plastic-grease combination was PA66 with Grease A which had the second worst wear performance with a maximum wear depth of 16.4 μm after 1M cycles along with the highest average friction coefficient of $\bar{\mu} = 0.037$. With $\bar{\mu} = 0.035$ and a wear depth of 19.4 μm , PA46 with Grease A was deemed equally bad for the application in hand.
- Grease D had the overall best performance of any of the greases with three out of the five lowest $\bar{\mu}$ values out of the twelve material-grease combinations, the best wear overall wear performance of any material-grease pairing (when used with PEEK), and favorable wear performances with PA46 and PA66.

4.3 Recommendations for Future Work

The following list details several possible areas in which future research could be conducted to expand upon this study and improve upon the work that was conducted:

- Expand the number of materials that are tested. Various other polyamides (e.g. PA6 and PA12) could be investigated since previous research has shown the performance of PA6 and PA12 to be comparable to the PA46 and PA66 tested in this study. There are also additional materials such as POM (acetal) that could be investigated, especially for lightly loaded applications.

- Examine the effects of different fillers such as molybdenum disulphate and aramids, the percentage of filler used, and the length of the fibers.
- Expand the number of greases tested and examine the relationship between the grease properties and the traction and wear performance. A study using nonproprietary greases would be able to better examine the effect of the grease properties.
- Perform tests at other operating conditions to expand the database. Traction tests with different normal loads F_n and rolling velocities u_r and wear tests at different slide-to-roll ratios R , F_n , and u_r can be performed for this purpose.
- The test setup can be improved significantly by devising a real-time disk surface temperature measurement system such that possible relationships between temperature increases and wear rate can be explained quantitatively.
- Method of application of grease to the contact interface can be improved by devising a way of continually lubricate the roller-disk contact with grease. Enclosing the interface of the roller and disk would allow for more consistent lubrication, though it would make accurate torque measurements more difficult during traction testing due to the increased drag from the grease.
- Before the results of this study can be considered in an actual product, it is advisable to perform lab experiments using actual gear drives to verify that the results from the twin-disk tests apply to gears as well.

REFERENCES

- [1] Wellenzohn, M., “Improved Fuel Consumption through Steering Assist with Power on Demand”, SAE Technical Paper Series, Paper 28, 2008
- [2] Liou, J.J., “A Theoretical and Experimental Investigation of Roller and Gear Scuffing,” PhD Dissertation, The Ohio State University, Columbus, Ohio, 2010
- [3] Harpster, S., “A Feasibility Study on Development of Dust Abrasion Resistant Gear Concepts for Lunar Vehicle Gearboxes,” MS Thesis, The Ohio State University, Columbus, Ohio, 2009
- [4] Chen, Y.K., Kukureka, S.N., and Hooke, C.J., “The wear and friction of short glass-fibre-reinforced polymer composites in unlubricated rolling-sliding contact”, *Journal of Material Science*, **31**, pp. 5643-5649, 1996.
- [5] Kukureka, S.N., Hooke C.J., Rao M., Liao, P., and Chen, Y.K., “The effect of fibre reinforcement on the friction and wear of polyamide 66 under dry rolling–sliding contact”, *Tribology International*, **32**, pp. 107-116, 1999
- [6] Chen, Y.K., Modi, O.P., Mhay, A.S., Chrysanthou, A., and O’Sullivan, J.M., “The effect of different metallic counterface materials and different surface treatments on the wear and friction of polyamide 66 and its composite in rolling–sliding contact”, *Wear*, **255**, pp. 714-721, 2003.
- [7] Clerico, M., “A Study of the Friction and Wear of Nylon against Metal”, *Wear*, **13**, pp. 183-197, 1969.
- [8] Gordon, D.H. and Kukureka, S.N., “The wear and friction of polyamide 46 and polyamide 46/aramid-fibre composites in sliding–rolling contact”, *Wear*, **267**, pp. 669-678, 2009.

- [9] Vaziri, M., Spurr, R.T., and Stott, F.H., "An Investigation of the Wear of Polymeric Materials", *Wear*, **122**, pp. 329-342, 1988.
- [10] Thorp, J.M., "Friction of Some Commercial Polymer-based Bearing Materials against Steel", *Tribology International*, **15**(2), pp. 69-74, 1982.
- [11] Cirino, M., Friedrich, K., and Pipes, R.B., "Evaluation of Polymer Composites for Sliding and Abrasive Wear Applications", *Composites*, **19**(5), pp. 383-392, 1988.
- [12] Yamamoto, Y. and Hashimoto, M., "Friction and Wear of Water lubricated PEEK and PPS Sliding Contacts, Part 2. Composites with Carbon or Glass Fibre", *Wear*, **257**, pp. 181-189, 2004.
- [13] Werner, P., Altstädt, V., Jaskulka, R., Jacobs, O., Sandler, J.K.W., Shaffer, M.S.P., and Windle, A.H., "Tribological Behaviour of Carbon-nanofibre-Reinforced Poly(ether ether ketone)", *Wear*, **257**, pp. 1006-1014, 2004.
- [14] Mao, K., Li, W., Hooke, C.J., and Walton, D., "Friction and Wear Behaviour of Acetal and Nylon Gears", *Wear*, **267**, pp. 639-645, 2009.
- [15] Kurokawa, M., Uchiyama, Y., and Nagai, S., "Performance of Plastic Gear Made of Carbon Fiber Reinforced Poly-ether-ether-ketone", *Tribology International*, **32**, pp. 491-497, 1999.
- [16] Kurokawa, M., Uchiyama, Y., and Nagai, S., "Performance of Plastic Gear Made of Carbon Fiber Reinforced Poly-ether-ether-ketone: Part 2", *Tribology International*, **33**, pp. 715-721, 2000.
- [17] Van Melick, H.G.H. and Van Dijk, H., "High-Temperature Testing of Stanyl Plastic Gears: A Comparison with Tensile Fatigue Data," *Gear Technology*, pp. 59-65, March/April, 2010.
- [18] Predki, W. and Pech, M., "Investigation of Load capacity for Crossed Helical Gears with Material Pairing of Steel/plastic", Proceedings of International Conference on Gears, pp. 75-86, Munich, Germany, 2010.

- [19] Predki, W. and Miltenovic, A., “Comparison of the Wear Load Capacity of Crossed Helical Gears with Wheels of Sinter and Plastic”, Proceedings of International Conference on Gears, pp. 35-46, Munich, Germany, 2010.
- [20] Kurokawa, M., Uchiyama, Y., Iwai, T., and Nagai, S., “Performance of Plastic Gear Made of Carbon Fiber Reinforced Polyamide 12”, *Wear*, **254**, pp. 468-473, 2003.
- [21] Adams, Clifford E., “Plastics Gearing,” Marcel Dekker, Inc., 1986
- [22] Victrex PEEK, Victrex PEEK 450CA30, Retrieved January 30, 2011 from http://drakeplastics.com/msds/VictrexPEEK450CA30_en.pdf
- [23] Young, Warren C. and Budynas, Richard G., “Roark’s Formulas for Stress and Strain,” McGraw-Hill, 2002
- [24] Stanyl by DSM, Stanyl TW200FS, Retrieved March 1, 2012 from <http://www.sheng-yu.cn /upload/20091027175202.pdf>
- [25] SABIC Innovative Plastics, Data Sheet Comparison, Retrieved March 1, 2012 from http://www.sabic-ip.com/gepapp/eng/datasheetinter/compare?click=1002002000_1002003093_1002036227&sltUnit=0
- [26] MatWeb, AISI 4620 Steel, Retrieved March 2, 2012 from <http://www.matweb.com/search/datasheet.aspx?matguid=d5670187e40947908b4a4e8ce19c7931&ckck=1>